ANL/ESD-14/18

Developing County-Level Water Footprints of Biofuel Produced from Switchgrass and *Miscanthus* × *Giganteus* in the United States

Energy Systems Division

ANL/ESD-14/18

Developing County-Level Water Footprints of Biofuel Produced from Switchgrass and *Miscanthus* × *Giganteus* in the United States

by
May Wu and Yi-Wen Chiu
Energy Systems Division, Argonne National Laboratory

September 2014

CONTENTS

FIGURES

TABLES

NOMENCLATURE AND ABBREVIATIONS

AET	Actual evapotranspiration
BM	Biomass (cellulosic) growth potential (kg/m^2/month)
BGI	Blue and green water resource index
BT2	U.S. Billion-Ton Update
Ecan	Rain captured and evaporated from the grass canopy
EISA	Energy Independence and Security Act
Es	Evaporation from soil
ET	Evapotranspiration
ETo	Reference evapotranspiration
Fc	Field capacity
HUC	Hydrologic unit code
IPAR	Intercepted photosynthetically active radiation
LAI	Leaf area index
LSWG	Switchgrass, lowland ecotype
MMT	Million metric tons
MXG	*Miscanthus* × *giganteus*
NOI	Nitrogen fertilizer application-loading ratio (weight/weight)
Pw	wilting point
RainD	Average raining days in a given month
R_{IPAR}	Intercepted photosynthetically active radiation
Rn	Net solar radiation
RUE	Intercepted radiation use efficiency
SunD	Average sunny days in a given month
SWAT	Soil water analysis tool, a watershed model
SWG	Switchgrass
TP	Vegetation transpiration
USDA	U.S. Department of Agriculture
USDOE	U.S. Department of Energy
USGS	U.S. Geological Survey
USWG	Switchgrass, upland ecotype

Ws	Water balance in the soil compartment
WUE	Water use efficiency

ACKNOWLEDGMENTS

This work was made possible by funding from the U.S. Department of Energy, Bioenergy Technologies Office (BETO), Office of Energy Efficiency and Renewable Energy, under contract # DE-AC02-06CH11357. We would like to thank Kristen Johnson of BETO for her valuable inputs and suggestions throughout the study.

Developing County-Level Water Footprints of Biofuel Produced from Switchgrass and *Miscanthus* × *Giganteus* in the United States

May Wu and Yi-Wen Chiu
Energy Systems Division, Argonne National Laboratory, Argonne, IL

EXECUTIVE SUMMARY

Perennial grass has been proposed as a potential candidate for producing cellulosic biofuel because of its promising productivity and benefits to water quality, and because it is a non-food feedstock. While extensive research focuses on selecting and developing species and conversion technologies, the impact of grass-based biofuel production on water resources remains less clear. As feedstock growth requires water and the type of water consumed may vary considerably from region to region, water use must be characterized with spatial resolution and on a fuel production basis.

This report summarizes a study that assesses the impact of biofuel production on water resource use and water quality at county, state, and regional scales by developing a water footprint of biofuel produced from switchgrass and *Miscanthus* × *giganteus* via biochemical conversion. Estimates of the blue,[1] green,[2] and gray[3] water footprints of these perennial biofuels were conducted at the county level for the U.S. On the basis of the feedstock resource production potential projected in the U.S. Billion-Ton Update [USDOE 2011], a series of feedstock production scenarios is analyzed. The perennial-grass-based biofuel pathway is examined under six biomass resource projection scenarios, for the years 2022 and 2030 at farm-gate prices of $40, $60, and $80 per dry short ton of feedstock. The results show that the blue water footprint of biofuel produced from perennial grass ranges from 2.65 to 5.40 L of water per L of biofuel (L L^{-1}) on the county level, with a production-weighted average between 4.22 L L^{-1} and 4.52 L L^{-1}. The county-level green water footprint falls between 529 and 3,106 L L^{-1}, with an average between 1,091 L L^{-1} and 1,170 L L^{-1}. Gray water ranges from 0.06 up to 602 L L^{-1} with an average between 27 L L^{-1} and 33 L L^{-1}. This gray-water footprint range is comparable to that of biofuel based on forest wood resources. The intensity of green and gray water footprints for the three feedstocks studied can be ranked as USWG > LSWG > MXG. The state, regional, and national water footprints associated with each type of grass can fluctuate under different feedstock production scenarios as a consequence of spatial aggregation of land conversion. Green and gray water footprints increase in the highest biomass production scenarios for year 2022 and 2030. On a per liter biofuel production basis, there is no clear and consistent pattern in water footprint for

[1] The blue water footprint represents all the consumptive water that is withdrawn from surface water and groundwater for use in feedstock irrigation and refinery processing.

[2] The green water footprint represents the portion of feedstock water demand that is satisfied by soil moisture from precipitation during the growing stage.

[3] The gray water footprint represents the water required to assimilate the pollutant load so it meets an acceptable concentration standard in streams.

the production regions in the U.S. across the six scenarios studied. This study illustrates the county-level water footprints associated with biofuel production from perennial grasses, highlights the interconnection between land use and water footprints, and demonstrates the geographical deviations of water footprints under different feedstock production scenarios.

1 INTRODUCTION

The proposal to use perennial grass as an energy crop in the United States dates back to the 1970s [Hohenstein and Wright 1994], when it was considered primarily for power generation. With the advantages of high adaptability, high yields, nutrient turnover, and little carbon debt and food competition [David and Ragauskas 2010; Fargione et al. 2008], perennial grass has also been proposed as a cellulosic feedstock candidate to increase U.S. green fuel production [USDOE 2011; McLaughlin and Kszos 2005]. Of the perennial species, *Miscanthus* (*M.* × *giganteus* or MXG) and switchgrass (*Panicum virgatum* or SWG) have gained particular attention, owing to successful experiences in Europe and their long history of use as forage [Heaton et al. 2010; Lewandowski et al. 2000]. Previous field trials established in the State of Illinois in the United States indicate that the yields of SWG and MXG can be 2.7 and 7.8 times higher, respectively, than those of other low-input, high-diversity prairie systems [Heaton et al. 2008]. MXG and an ecotype of hybrid SWG even appear to have 1.7 and 1.2 times higher biomass yield than that of harvestable corn grain and stover combined [Heaton et al. 2008; Vogel and Mitchell 2008]. The lower land-resource requirement associated with high-yield energy crops is the primary motive to consider perennial grass as cellulosic feedstock for biofuel production [USDOE 2011]. From the life-cycle perspective, blending SWG biofuel into conventional transportation fuels can lead to significant reductions in greenhouse gas and critical pollutant emissions [Wu et al. 2006; Adler et al. 2007; Tilman et al. 2006] and achieve promising high-net-energy yield [Fargione et al. 2008; Schmer et al. 2008; Angelini et al. 2009]. Although perennial grasses such as SWG have been used in soil and water conservation programs, their overall water needs and their growth in various regions have not been systematically evaluated on a large scale.

In view of concerns about the effects of biofuel development on water sustainability [Berndes 2002; Fingerman et al. 2011, Dominguez-Faus et al. 2009], several studies were conducted to address the water use of perennial grasses by quantifying water use efficiency and hydrological effects on a local or experimental-lot scale [Hickman et al. 2010; Beale et al. 1999; Vanloocke et al. 2010; McIsaac et al. 2010; Nyakatawa et al. 2006; Glover et al. 2010]. These studies have laid an important foundation illustrating the role of perennial grass in altering the water cycle and confirmed that perennial grass can lower soil moisture, owing to its higher evapotranspiration (ET) compared with corn or wheat [Hickman et al. 2010; McIsaac et al. 2010; Glover et al. 2010]. To better support energy policies, it is necessary to better understand the effects of biofuel production on water resources from a life-cycle perspective. As shown in several recent studies [Chiu and Wu 2013; Wu et al. 2012; Chiu and Wu 2012], the water consumption associated with biofuel production must be determined on a local basis in order to reflect the variances of climate and biomass growth potentials.

Conceptually, the biofuel water footprint during the crop growing and refinery conversion stages can be partitioned into three compartments, i.e., green water, blue water, and gray water. Green water represents rainwater used to support crop growth through ET; blue water represents surface water and groundwater used by crops through ET and in the production of fuels, energy, and other goods. Gray water is defined as the volume of freshwater that is required to assimilate the load of nutrients/chemicals on the basis of water quality standards

established by the U.S. Environmental Protection Agency. Chapagain and Hoekstra [2004] proposed a water footprint accounting methodology for products, countries, and regions. The key elements of the methodology have been incorporated into ISO 14046 standard [ISO 2014] as a stand-alone life cycle assessment for water impact or a part of a comprehensive LCA of environmental impacts. A recent review [Wu et al. 2014] summarized studies attempted to estimate water requirements across the major stages of the biofuel supply chain [Staples et al. 2013; Chiu and Wu 2013a, Chiu and Wu 2013b, Chiu and Wu 2012, Wu et al. 2012, Mishra and Yeh 2011; Scown et al. 2011; Wu et al. 2011b, 2009; Gerbens-Leenes et al. 2009; Gerbens-Leenes and Hoekstra 2009; Chiu et al. 2009; Evans and Cohen 2009; King and Webber 2008]. The feedstock analyzed by these researchers included grain, sugar crops, agricultural residue, herbaceous grass, and forest wood. Effort has been made to establish water footprints of biofuels produced from corn, soybean, agricultural residue [Chiu and Wu, 2012] and forest wood resources [Chiu and Wu 2013a] in the U.S. at the county level. The water footprint of algae-based biodiesel for the 17 southern states in the U.S. was also reported [Chiu and Wu 2013b]. The approach of incorporating watershed modeling into the water footprint shows improved spatial resolution in describing water quality change [Wu et al. 2012]. Needs and water issues associated with various stages of biofuel production is being regularly reviewed [McIsaac 2014].

2 SCOPE OF THE STUDY

This work aimed at developing water footprints of biofuel produced from SWG and MXG in the United States. To reflect the regional variability of climate, soil, and crop growth, a key focus was characterizing water use with a county-level spatial resolution. We examined water consumption at major life-cycle stages—from growing feedstock on farms to producing biofuel in biorefineries. As the production pathway is not yet commercialized, this study derived its biomass resource production scenarios from current research and future projections. Water footprints were classified into three types: blue, green, and gray water. The blue water footprint accounts for all the consumptive water from feedstock irrigation and refinery processing. The green water footprint is the portion of feedstock water demand satisfied by precipitation during the growing stage. The gray water footprint represents the water required to assimilate the pollutant load in order to meet an acceptable concentration standard in streams [Hoekstra et al. 2011]. The blue, green, and gray water volumes associated with each liter of biofuel production (in $L\ L^{-1}$) are presented on a county and regional level in order to show the spatial variances and compare scenarios. With this approach, the biofuel water impacts associated with perennial grass on a regional scale as well as through the biofuel production life cycle can be quantified.

3 SCENARIOS

This study focuses on three types of perennial feedstock: MXG, lowland-ecotype SWG (LSWG), and upland-ecotype SWG (USWG). The perennial biomass production is analyzed on the basis of current yield and projections. A biomass resource assessment, commissioned by the United States Department of Energy [USDOE 2011], provides an estimate of agricultural and forest resources in terms of market prices, soil productivity, erosion control, and other parameters. The assessment ― the U.S. Billion-Ton Update (BT2) ― projects that at least one billion dry tons of biomass can be produced annually within the contiguous United States in a sustainable manner. This amount of biomass will be available by 2030 for biofuel production to displace approximately 30% of the country's present petroleum consumption, given various assumptions of current and future inventory and production capacity, availability, and technology advancement. For the present study, six of the cellulosic feedstock production scenarios discussed in BT2 were selected, using farm-gate prices of $40, $60, and $80 (in U.S. dollars) per dry ton and the U.S. Department of Agriculture (USDA) baselines for 2022 and 2030. The scenarios give a total biomass production tonnage from perennial grass feedstock at the county level (Table 1).

Table 1 Cellulosic biomass production from perennial grasses under projected scenarios

Scenario	YR2022/ 40	YR2022/ 60	YR2022/ 80	YR2030/ 40	YR2030/ 60	YR2030/ 80
Farm-gate price	$40	$60	$80	$40	$60	$80
Perennial Biomass (MMT)	11	171	224	27	231	274

4 METHOD AND DATA SOURCES

Figure 1 presents the system boundary for this study and the calculation steps taken to derive the water footprints for perennial biofuels. A critical step in estimating blue and green water is determining the growth yield of the feedstock crops. Initially, the perennial growth potential in various geographical regions is calculated on the basis of meteorological data and grass-specific growth parameters. The grass production is then compared with the distribution of biomass-producing counties projected by the BT2 report [USDOE 2011] in each future scenario. Results are further screened to select the dominant grass type at the county level and determine the required harvest acreage. Water requirements during the feedstock growing stage are based on the plants' ET. Water use in the biorefinery stage is estimated on the basis of process knowledge. Gray water accounting is limited to nitrogen fertilizer use. Because there is little water use when biofuel is transported to refueling station and combusted in vehicle engines, the life-cycle water footprint for the perennial biofuel production pathway is a summation of water use during the feedstock-growing and refining stages. This work follows a conceptual water footprint accounting flow for green, blue, and gray water in the biofuel production life cycle,

which is presented elsewhere [Chiu and Wu, 2012; Wu et al. 2012] [Gerbern-Lees et al 2009]. In this section, data sources and the methodologies employed to determine perennial grass growth potential, ET, selection of feedstock type, land area, and water use in the grass growth and conversion stages will be presented.

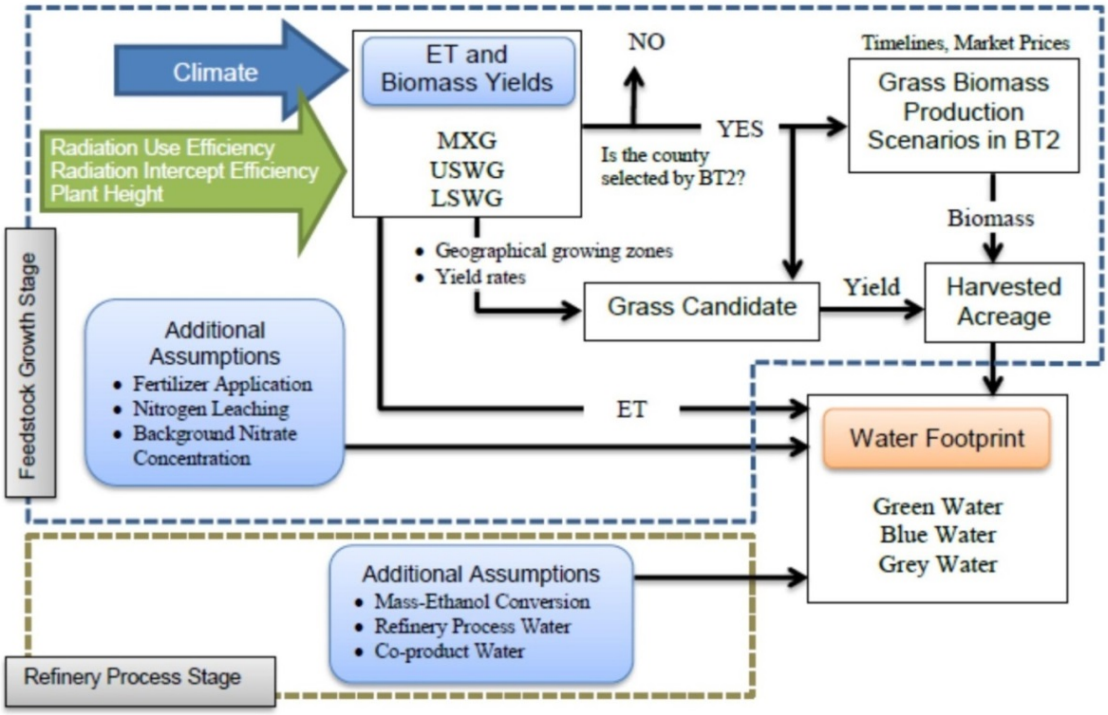

Figure 1 System boundary and calculation flows. ET – evapotranspiration; MXG – *Miscanthus* × *giganteus*; USWG – upland switchgrass; LSWG – lowland switchgrass.

4.1 Biomass Production Potential

MXG, USWG, and LSWG are selected as perennial grass feedstocks for generating cellulosic biofuel. Previous studies [Jager et al. 2010; Miguez et al. 2012] attempted to project perennial grass yields across the U.S. on an annual basis. However, because of changes in plant height and foliage over the growing season, which can affect crop ET and therefore water use, we calculated ET and biomass growth together in monthly steps to represent the growth patterns of distinct grass types with temporal resolution. The ET and biomass growth potential of each type of grass are estimated separately on the basis of the climate conditions of each county in the lower 48 states of the U.S.

4.1.1 Perennial Biomass Growth

We estimated grass biomass production potential at the county level for MXG, USWG, and LSWG on the basis of growth parameters and climate conditions. Grass biomass yield can be estimated by employing the equation adopted in earlier studies [Heaton et al. 2008; Neitsch et al. 2011; Jager et al. 2010; Miguez et al. 2012, Price et al. 2004], which gives yield as a function of radiation and the efficiencies of radiation use and interception by each type of grass. We assume that growth begins whenever temperature permits and ends in November, when harvesting takes place. U SWG, LSWG, and MXG reach maximum heights of 150, 250, and 320 cm [USDA NRCS 2012], respectively, in October. To estimate grass biomass (BM, in kg/m^2/month) under given climate conditions, we employ equations [1-3]:

$$BM = RUE \times R_{IPAR} \times \varepsilon_i \quad , \tag{1}$$

where

- RUE, discussed further below, is the intercepted radiation use efficiency (g per MJ IPAR),
- R_{IPAR} is the intercepted photosynthetically active radiation (MJ/m^2/month), and
- ε_i is the plant's radiation intercepting efficiency.
- In general, the value of R_{IPAR} is found to be 0.460 to 0.501 of the incident shortwave radiation [Jacovides et al. 2003]; therefore, we assume the average value of 0.45 in this study.
- The plant radiation intercepting efficiency ε_i can be calculated as

$$\varepsilon_i = 1 - \exp(-K \times LAI) \quad , \tag{2}$$

where

- K is the radiation extinction coefficient, with a value of 0.33 [McLaughlin et al. 2006] and
- LAI is the leaf area index, calculated from vegetation height (H, in cm) in a given month [Neitsch et al. 2011];

$$LAI = 1.5 \times LN(Hc) - 1.4 \tag{3}$$

RUE can differ widely among different grasses owing to climate and growing season [Zegada-Lizarazu et al. 2012]. After comparing available field data and literature reports [Hohenstein and Wright 1994; Kiniry et al. 2012; Miguez et al. 2012; Gunderson et al. 2008; Dohleman et al. 2012], we assume the following RUE values for the peak growing phase (March to late July):

- USWG: 3.17, average yield 5.26 dst/ac

- dst/ac: dry short ton per acre of land
- LSWG: 3.34 (range 2.16~5.10), average yield 5.76 dst/ac
- MXG: 2.38 (range 1.25~3.71), average yield 8.97 dst/ac

As most of the RUE values are measured during peak growth season (around June or July) to estimate biomass growth on an annual basis, we have to take temporal variation of RUE into account in computing the monthly growth pattern. A previous study [Nouvellon et al. 2000] found that the RUE in the early growing season is about 8.75 times higher than in the late growing season. Therefore, we assume that the RUE values in May (SWG) and June (MXG) are 20% and 50%, respectively, of what is observed in peak season, and the RUE value afterward is 11% of the peak value. To generate the spatial deviation of RUE, the county-level RUE factors are derived by comparing the local annual yield (Y_{county}) estimates for SWG and MXG from the literature [Lewandowski et al. 2000; Miguez et al. 2012] with the average field measurement (Y_{ref}) [Adler et al. 2007; Dohleman et al. 2012]. Thus,

$$RUE_{county} = RUE_{ref} \times \frac{Y_{county}}{Y_{ref}} \quad (4)$$

4.1.2 Climate Criteria

On the basis of literature values, the following temperature and precipitation criteria were established to screen for counties that are suitable as growing locations for MXG and SWG:

- MXG shoots emerge and leaf extension occurs at temperatures >10°C, compared to >12°C for other C4 grasses.[4]
- Winter temperatures lower than −3.4°C can kill 50% of MXG plants [Heaton et al. 2010]. We set the minimum temperature for MXG at −17°C.
- MXG requires over 500 mm of water during the growing season [Heaton et al. 2010]. Therefore, a county that normally receives less than 500 mm of rain from April to September would be classified as an unsuitable location for growing MXG, and hence is eliminated from the map.
- For SWG, the required winter temperature is >−17°C, and the growing-season precipitation >310 mm [Jager et al. 2010].
- Upper temperature limits for growth were also selected. A previous study indicated that LSWG and USWG will stop growing at temperatures >25°C and >24°C, respectively [Gunderson et al. 2008]. The work of Naidu et al. [2003] suggests that at a threshold of 30°C, MXG starts to show growth reduction. To simulate a reasonable growth pattern, for each month of the growing season, we assumed the plants would grow slowly (at 50% of the peak rate) if the temperature reached the upper limits.

[4] Plants use a supplementary method of CO_2 uptake which forms a 4-carbon molecule.

4.1.3. Biomass Loss

During harvesting and feedstock transportation, a portion of the available biomass can be lost. Field machinery would leave 10 cm of crop stems in the fields after harvest. The biomass loss could be as high as 30%~50%, with an average 33% for MXG [Heaton et al. 2010] and 17% for SWG [Heaton et al. 2008]. We assume a 15% loss, taking into consideration the likely improvements in harvesting practices and packaging technology by 2022 and 2030.

4.2 Estimating County-Level Production and Land Requirements

On the basis of the distribution zone of native regions for perennial grasses [USDOE 2006], we applied the six scenarios (Table 1) as geographical screening layers, spatially filtering out the designated feedstock-producing counties and their corresponding biomass production. We determined the most suitable grass type on the basis of the geographical growth zones of MXG, USWG and LSWG, and its yield on the basis of perennial growth modeling. If a selected county is located in a region suitable for growing all three types of grass, the one with the highest yield would be the dominant feedstock candidate for this county.

Together with the projected biomass production in the county (Section 3) and the local estimated grass yield (Sections 4.1.1.−4.1.2), the acreage of appropriated land for growing grass can be determined. It is assumed that the grass feedstock will be grown in non-crop areas, which are defined in this study as areas of idle land, pasture, hay, alfalfa, and grassland. The land appropriation for perennial feedstock cannot exceed the total non-crop land in a county. Therefore, a county's land appropriated for grass biomass production is capped at the total (100%) of the non-crop areas. Available biomass feedstock production is further adjusted accordingly.

4.3 Perennial Grass Evapotranspiration

MXG, LSWG, and USWG all have distinct ET rates and growth patterns. To estimate actual ET (AET) from perennial grassland, this study considered ET losses from three major components: rain captured and evaporated from the grass canopy (E_{can}), vegetation transpiration (TP), and evaporation from soil (Es). The sum of these three components is defined as the AET of grasslands. The computation procedure is adopted from the soil water analysis tool (SWAT) model [Neitsch et al. 2011], using Penman-Monteith [Allen et al. 1998] potential ET. The required climate input data (temperature, precipitation, solar radiation, and wind speed) are available as average values between 1970 and 2000. It is assumed that ET patterns will remain the same as in the past through 2030. Thus, the historical climate "norm" estimated by using the current climate dataset (1970–2000) is applicable.

The AET and its three components were computed in monthly steps by incorporating thirty-year monthly input data for average climate (temperature, precipitation, solar radiation, humidity, and wind speed). Key parameters and calculation steps are listed below.

- **Rain captured and evaporated from grass canopy (E_{can}):**

$$E_{can} = if\ AvgT < 0{,}0, else \\ if\ ET_0 < 0.0004 \times LAI \times 1000 \times RainD, ET_0, else \\ 0.0004 \times LAI \times 1000 \times RainD \quad (5)$$

where

- $AvgT$ is the average monthly temperature (°C), using monthly maximum and minimum temperature as inputs,
- ET_0 (mm/month) is the reference ET (mm/month),
- *LAI* is the leaf area index, estimated from plant height, and
- $RainD$ is the average raining days in a given month.

$$ET_0 = \max(0.01, \left[\frac{\Delta \times Rn + \gamma \times (1710 - 6.85AvgT) \times (es - ea)/r_a}{\Delta + \gamma \times \left(1 + \frac{r_c}{r_a}\right)} \right] / \lambda) \times SunD \quad (6)$$

It is assumed that ET_0 < 0.01 mm/month is not detectable by a field instrument. Therefore, the lowest ET_0 value would be 0.01 mm. The input parameters in eq. (6) are defined as follows:

- Δ is the slope of saturated vapor pressure,
- *Rn* is the net solar radiation (MJ/m^2/day),
- γ is the psychrometric constant (kPa/°C),
- *es – ea* is the difference in vapor pressure (kPa),
- r_c is the canopy resistance (s/m),
- r_a is the aerodynamic resistance (s/m),
- λ is the latent heat of vaporization (MJ/kg), and
- *SunD* is the number of sunny days = day count in a given month – *RainD.*

- **Vegetation transpiration (TP):**

$$TP = if\ LAI \leq 3, (ET_0 - E_{can}) \times LAI/3, else\ ET_0 - E_{can} \quad (7)$$

The calculation is completed by linking the estimates of plant *LAI*, ET_0, and E_{can} on a monthly basis. The *LAI* calculation is presented in eq. (3).

- **Evaporation from soil (E_s):**

$$E_s = \min(E'_{s\,adj}\ , 0.8 \times (W_s - P_w)) \quad (8)$$

where

- E_s is the amount of water evaporated from soil (in mm),
- $E'_{s\,adj}$ is adjusted evaporated demand (in mm),
- W_s is water content in the soil layer (in mm),
- P_w is wilting point (in mm).

The value of W_s fluctuates over time owing to ET, and P_w is defined by the local soil type. Together with the water content and wilting point, the evaporated demand (E'_s) can be adjusted ($E'_{s\,adj}$):

$$E'_{s\,adj} = E'_s \times \exp\left(\frac{2.5(W_s - F_c)}{F_c - P_w}\right) \qquad if \quad W_s < F_c\,, else\ E'_{s\,adj} = E'_s \tag{9}$$

$$E'_s = E''_s \times \left[\frac{100}{100+\exp(2.374-0.00713\times 100)} - \frac{10\times 0.95}{10+\exp(2.374-0.00713\times 10)}\right] \tag{10}$$

$$E''_s = \min\left[(ET_0 - E_{can}) \times \exp\left(-5\times 10^{-5}\times M_{grass}\right),\ \frac{(ET_0 - E_{can}) \times \exp\left(-5\times 10^{-5}\times M_{grass}\right) \times (ET_0 - E_{can})}{(ET_0 - E_{can}) \times \exp\left(-5\times 10^{-5}\times M_{grass}\right) + TP}\right]$$

$$E''_s = 0, \ \ if\ AvgT < 0\ or\ ET_0 - E_{can} = 0 \tag{11}$$

where

- Fc is field capacity (in mm),
- M_{grass} is the plant coverage (kg/ha) on the soil.

Thus, soil evaporation must be linked with the grass growth model in the corresponding monthly step. M_{grass} is the accumulated BM up to the simulated month. Monthly data for biomass growth were introduced into the AET calculation, providing the required input parameters simulating land cover change over time. M_{grass} in December would be 0, as grass is scheduled to be harvested at the end of November in our study.

The water content in soil compartment at start of month t is then computed as

$$W_{s\,t+1} = W_{s\,t} + Prcp_t - AET_t \tag{12}$$

$$Pw \le W_{s\,t+1} \le Fc$$

It is assumed for modeling purposes that 15% of the soil water remains in the soil layers in the first month as a seed.

Thus, $Ws_0 = Pw + 0.15(Fc - Pw)$

During the low-ET months (when the reference ET, ET_0, is less than the free water held in the canopy layer), we assume that the actual evaporation would equal canopy evaporation E_{can} [eq. (5)]; hence, $E_{can} = ET_0$. Thus, the following equation applies:

$$AET = if\ ET_0 < 0.0004 \times LAI \times 1000 \times RainD, ET_0 \quad else\ E_{can} + TP + E_s \qquad (13)$$

The green water volume is then determined by multiplying the AET (mm) by the land area of its corresponding grass type.

Estimated AET for the grasses is further compared with remote sensing measurements of pasture land to verify the computation quality based on the similarity between the two [Hickman et al. 2010; De La Torre Ugarte et al. 2010]. Therefore, satellite imagery derived ET data layers from 1983 to 2006 obtained from the Numerical Terradynamic Simulation Group at the University of Montana [NTSG 2012] are compiled and overlap with US crop data layers [USDA 2010] to identify the location of hay/pasture lands. The satellite ET occurring on hay/pasture lands in the U.S is extracted and calculated the average satellite grass ET. Finally the spatial data were converted to county level for comparison with the estimated ET data from this study.

4.4 Blue Water

Water footprint accounting quantifies three key water components: blue, green, and gray water. Green water is determined by local effective precipitation, and blue water by ET [Hoekstra et al. 2011, Wu et al. 2012] and process water use in the biorefinery. In the biorefinery, the perennial grass feedstock is converted to biofuel via a biochemical process, in which 5.4 liters of processing water is required to produce a liter of biofuel. Bioelectricity is generated as a co-product from the process at a rate of 1.8 kW per gallon of biofuel produced [Humbird et al. 2011]. The bioelectricity is used to displace electricity from the grid. Therefore, the water consumed during the generation of bioelectricity can be saved as a credit. On the basis of a previous assessment of state-level water consumption for electricity generation [Wu and Peng 2011], each liter of biofuel production receives 0.07 to 2.75 liters of water credit for displacing grid electricity in perennial grass-growing states.

4.5 Gray Water

Gray water is the water-footprint indicator quantifying a production system's effects on water quality. This study focused on nitrogen-associated gray water, not only because nitrogen is suggested as an indicator in the *Water Footprint Assessment Manual* [Hoekstra et al. 2011], but also because it is the largest non-point source of pollutant from agricultural land. Given the magnitude of environmental impacts that result from nitrogen leaching, nitrate is one of the compounds extensively monitored and regulated by the U.S. Environmental Protection Agency to ensure a safe drinking water supply and to sustain ecological services [USEPA 1992].

Although using nitrogen-associated gray water may not comprehensively illustrate the full range of impacts induced by a production system, it provides a direct insight that puts fertilizer application into perspective. Gray water is calculated as a function of fertilizer use and process wastewater discharge; thus, it requires data for fertilizer input, nitrate leaching, and the natural background nitrate concentration. However, large-scale research on nitrogen loading in response to application of SWG and MXG fertilizer is still lacking. Results derived from previous field studies conducted in Alabama, Illinois, Kentucky, Minnesota, Pennsylvania, and South Dakota indicated that SWG appears to have an average nitrogen uptake efficiency 1.71 times higher than alfalfa [Huang et al. 1996; Stout 1992; Collins 1994; Schmitt et al. 1994]. There are few studies that directly compare MXG and alfalfa with regard to nitrogen uptake efficiency. On the basis of the literature values [Schmitt et al 1994; Christian et al. 2008], we estimated that MXG's nitrogen uptake efficiency is approximately 1.97 times higher than that of alfalfa. We applied these factors and assumed that nitrogen loading from SWG and MXG lands is 67% and 97% less than alfalfa, respectively, to adjust the nitrogen fertilizer application-loading ratios (NOIs) of alfalfa. The NOIs were calculated on the basis of the 1992 watershed-level U.S. Geological Survey (USGS) data across the entire lower 48 states of the U.S. [USGS 2011]. The watershed-level values were then converted to county level by using the zonal statistics tool in ArcGIS. If the region/county value was not available, we assumed the region/county would apply fertilizer at the same rate as neighboring regions. Given annual fertilizer application rates ranging from 44.8 to 78.4 kg N per hectare of grassland, the nitrogen loading can be estimated by incorporating the approximated state level NOIs (Chiu and Wu 2012). The fraction of nitrate in total nitrogen leached is assumed to be 94% [Wu et al. 2012b].

4.6 Water Resource Sufficiency

To evaluate the impacts of grass biofuel on water resources, two indices, water use efficiency (WUE) and Blue and green water appropriation index (BGI), were adopted in this study. WUE quantifies the feedstock biomass harvested per unit of water consumed throughout the entire growing season. The BGI compares total amount of green and blue water required with annual precipitation in the production region.

4.7 Data Sources

To compute the ET of perennial grass, we derived climate data from the SWAT climate generator [Neitsch et al. 2011], averaging historical climate data recorded by the National Oceanic and Atmospheric Administration from 1970 to 2000. To quantify gray water, values for fertilizer and nitrogen loading are essential information. The fertilizer requirements, based on state soil characteristics, are available from the BT2 report [USDOE 2011]. The natural background nitrogen concentration was derived from a USGS study estimating nitrogen levels between 1976 and 1997 [Smith et al. 2003]. This dataset is in a hydrologic unit code (HUC-8) at watershed-level resolution which was converted to the county level. Perennial grass feedstock is assumed to grow on non-crop lands, including existing pasture, hay, alfalfa, grassland, and idle lands. The total area of these types of land covers was analyzed on a county basis by using the raster map of the 2010 Crop Data Layer of the U.S. [USDA 2010] for analysis purposes. We

assume the land cover scheme will remain the same in 2022 and 2030. The value of field capacity (Fc) of local soil comes from an Oak Ridge National Laboratory data set [ORNL 2011].

5 RESULTS AND DISCUSSION

5.1 Perennial Grass Yield

The potential biomass yield for SWG and MXG are modeled for ten USDA resource regions at the county level under 30-year historical climate conditions. The yields were aggregated to the region level and weighted by non-crop land area, including pasture, hay, alfalfa, grassland, and idle land. County-level perennial grass yield ranges from a trace to 19.0, 29.8, and 44.4 Mg ha-1 for USWG, LSWG, and MXG, respectively, with a weighted ten-region average of 5.9, 7.3, and 12.6 Mg ha-1 before taking harvest loss into account (Table 2). Results were further compared with those generated from annual-basis models [Jager et al. 2010; Miguez et al. 2012] in various regions. As indicated in Table 2, yields of the three perennial grass types agree well with previous assessments on the basis of area-weighted ten-region averages, with the exception of USWG, where this study estimated a slightly (6%) lower yield overall. USWG appears to be the least productive, while MXG is capable of achieving the highest yield among the three. The present yields are rather dispersed from region to region, in a similar trend to the literature values. Compared with previous estimates, yields of MXG, LSWG, and USWG tend be higher in southern regions (Appalachia, Southeast, Delta, and Southern Plains) and lower in northern regions (Northeast, Corn Belt, Lake States, and Northern Plains). These differences could be caused by differences in the climate data year and/or climate parameters. Results suggest that MXG and LSWG are the most suitable for growth in Appalachia, the Southeast, and the Delta.

Table 2 Estimated perennial grass yield (Mg ha-1) for ten regions in the U.S., from the literature and this study.[1]

Region	USWG[2]	LSWG[2]	MXG[3]	SWG[3]	USWG This study	LSWG This study	MXG This study
Northeast	12.2	9.8	19.4	8.2	8.9	7.6	15.5
Appalachia	12.9	17.1	20.7	9.4	13.4	18.8	22.3
Southeast	7.0	11.6	20.5	9.2	8.9	15.5	27.7
Delta	9.7	12.6	22.1	10.5	11.7	15.6	28.1
Corn Belt	12.5	15.1	23.6	10.9	11.0	14.0	22.8
Lake States	9.0	6.5	22.0	9.3	6.4	4.8	16.9
Northern Plains	7.8	7.5	13.5	6.0	6.4	6.6	12.0
Southern Plains	7.6	10.1	14.6	6.9	9.0	12.4	18.3
Mountain	1.2	1.1	3.3	2.0	1.0	1.0	2.4

Table 2 (Cont.)

Region	USWG[2]	LSWG[2]	MXG[3]	SWG[3]	USWG This study	LSWG This study	MXG This study
Pacific	0.5	0.2	4.1	2.3	0.4	0.2	3.7
Area-Weighted Average[1]	**6.3**	**7.1**	**12.4**	**5.8**	**5.9**	**7.3**	**12.6**

[1] Values are weighted by region-level available land including pasture, hay, alfalfa, grassland, and idle lands.

[2] Jager et al. 2010

[3] Miguez et al. 2012

5.2 Land Resource Requirements

The biomass production and land area required for the six scenarios are presented in Table 3. On the basis of the yield of the three perennial grass types, a dominant perennial feedstock type was selected for each county in the counties designated for growing perennial biomass under the six future scenarios [USDOE 2006]. Land areas required for cultivating the perennial feedstock were determined according to projected feedstock production tonnages in the counties. The land acquisition figures were further adjusted using available non-crop land area (see Section 4.2). The six production scenarios involve different distributions of counties with correspondingly different biomass production capacity. A total of 61 to 2,208 counties in the United States were considered, with a total perennial grass biomass production projected to range from 11 million to 267 million dry metric tons. Nationally, the feedstock-production scenarios require growing biomass on approximately 0.8 to 2.0 million hectares of land, which is equivalent to 14% to 20% of the total current non-crop lands (idle land, pasture, grass, hay, and alfalfa) in the counties delivering perennial feedstock (Table 3). The extent and intensity of non-crop land conversion can vary significantly depending on the future scenario (Figure 2, Figure 3). Geographically, the Southern Plains, Delta States, Appalachia, Southeast, and the southern part of the Northern Plains regions are the primary producers under the YR2030/80 scenario (Figure 2), whereas production is more limited in the central U.S. region in scenarios YR2022/40 and YR2030/40, as projected by the BT2 report [USDOE 2011]. The LSWG accounts for the biggest portion of the feedstock, producing 74% of grass biofuel under the $40 scenarios for both 2022 and 2030 (Fig. 3). SWG is likely to be outpaced by MXG from scenarios YR2022/40 to YR2022/80 and YR2030/40 to YR2030/80, with the increase in farm-gate prices (Figure 3). Meanwhile, the percentage of LSWG feedstock in total production decreases to 45% and 46%, respectively.

Table 3 Summary of land appropriation, biomass production, and biofuel production under the six BT2 production scenarios

		Scenario					
		YR2022/40	YR2022/60	YR2022/80	YR2030/40	YR2030/60	YR2030/80
Land Appropriated (%)[1]	USWG[2]	<0.01%	0.42%	1.21%	<0.01%	0.58%	1.97%
	LSWG[2]	13%	9%	8%	12%	12%	11%
	MXG[2]	3%	5%	5%	2%	7%	7%
	Total	**16.1%**	**15.1%**	**14.5%**	**14.2%**	**20.0%**	**20.6%**
Biomass[3] (MMT)	USWG	–	2	6	–	2	9
	LSWG	8	85	97	20	112	124
	MXG	3	79	115	7	109	134
	Total	**11**	**166**	**219**	**27**	**223**	**266**
Biofuel[3] (BL)	USWG	–	1	2	–	1	3
	LSWG	3	28	32	7	37	41
	MXG	1	26	38	2	36	44
	Total	**4**	**55**	**72**	**9**	**74**	**88**

[1] The land appropriation accounts for area growing perennial feedstock as a percent of total non-crop lands in those counties. The non-crop lands in this study include pasture, hay, alfalfa, grassland, and idle lands; the areas are 2010 estimates.

[2] Aggregated data represent three feedstock pathways: upland switchgrass (USWG), lowland switchgrass (LSWG), and *Miscanthus* × *giganteus* (MXG).

[3] Biomass production is in million metric tons (MMT), and biofuel production is in billion liters (BL).

Geographic distribution patterns of the perennial grass yield play a critical role in determining land appropriation for perennial feedstock, which affects green water use. MXG and LSWG are more likely to be the primary feedstocks in supporting cellulosic biofuel production. MXG can offer higher amounts of biomass production in some scenarios (Table 2), while consistently requiring smaller fractions of the land resources on a county and regional basis (Table 3). As biomass production volume increases from scenario to scenario, the feedstock growing area spreads to broader neighboring regions (Figure 2). Meanwhile, the feedstock mix shifts toward an increasing proportion of high-yield feedstock, such as MXG and LSWG (Table 3, Figure 3). Growing areas selected for USWG appear very limited—mostly in the Northern Plains region (Figure 2, Figure 3).

Evidently, the changes in feedstock mix translate to increased land use efficiency. Comparing scenario YR2022/80 to YR2022/60, biomass production increases 30% while land appropriation remains the same or even decreases. This change is even more drastic when one compares scenario YR2022/60 with YR2022/40; here, the biomass production increases 16-fold whereas land requirement decreases by 1% (Table 3). In this study, we placed an upper limit on land acquisition so that the land conversion would not exceed current total non-crop land area. With this constraint, the total biomass output decreases 0.3%–3.5% from the projected volume of the six scenarios. Imposing an upper limit of 50% of the total non-crop land area would further

reduce the projected biomass production by 3.7%–9%. Under the scenarios examined, a total area-weighted average of 2.15–2.39 m^2 of land area is required to produce a liter of cellulosic biofuel from perennial grasses. The lowest land use rates (2.15−2.17 m^2/L) are associated with the $60.00-per-dry-ton scenarios for both YR2022 and YR2030 (scenarios YR2022/60 and YR2030/60).

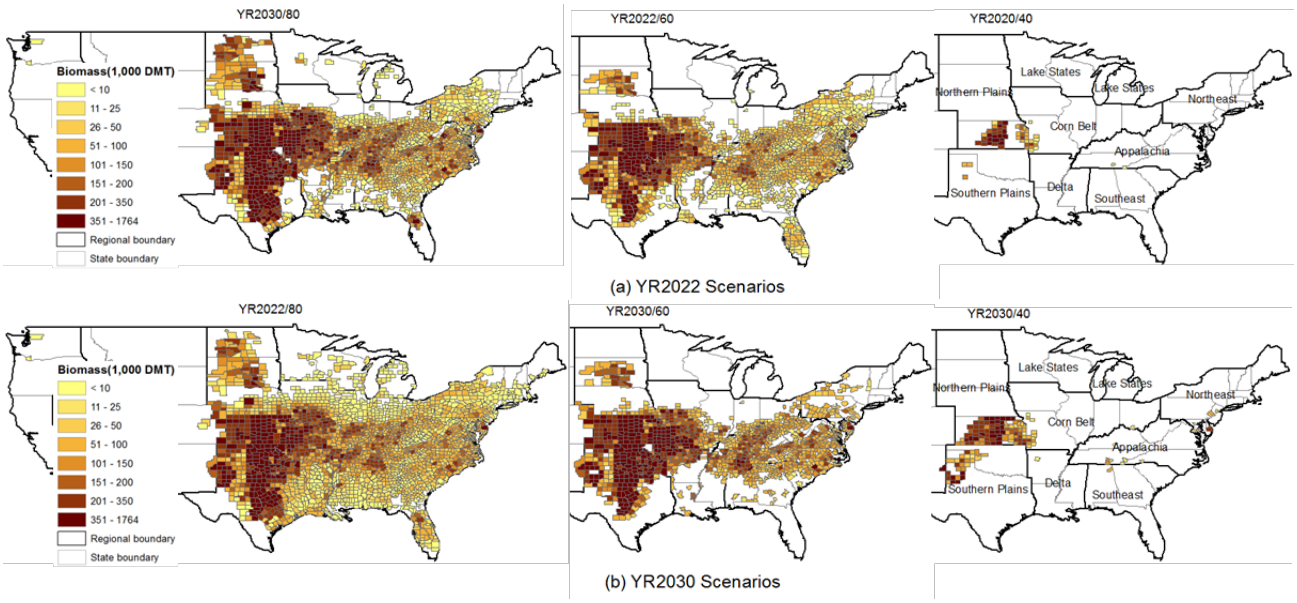

Figure 2 Spatial distribution of perennial biomass production in dry metric tons under proposed scenarios (USDOE 2011): (a) YR2022/40, YR2022/60, and YR2022/80; (b) YR2030/40, YR2030/60, and YR2030/80.

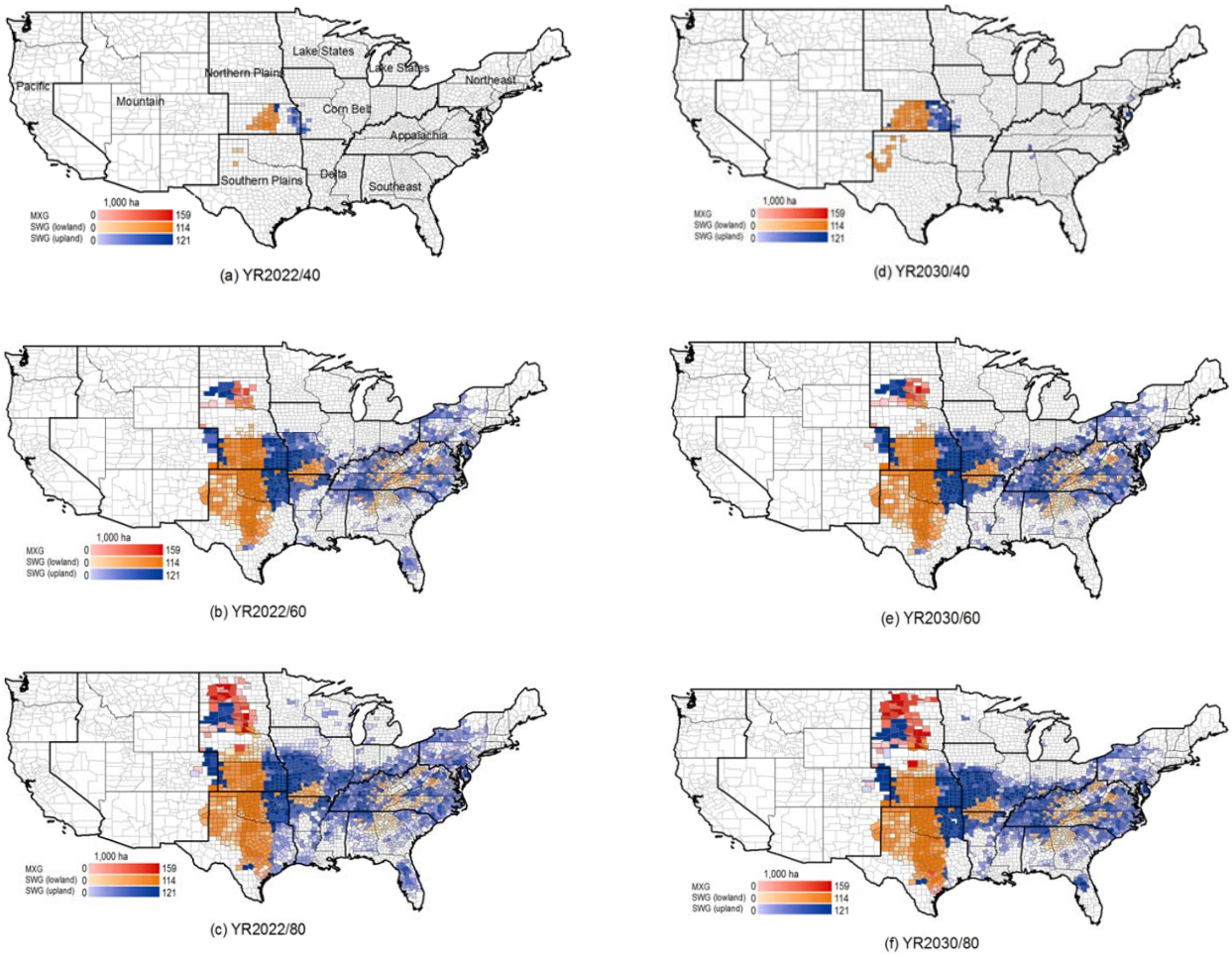

Figure 3 Distribution and acreage of grasslands designated for feedstock by type of species for six scenarios: (a) YR2022/40; (b) YR2022/60; (c) YR2022/80; (d) YR2030/40; (e) YR2030/60; (f) YR2030/80.

The levels of feedstock acquisition assumed under the six scenarios can lead to biofuel production between 4 billion and 88 billion L per year. To put these data into perspective, the Energy Independence and Security Act (EISA) mandates the production of 16 billion gal (61 billion L) of cellulosic biofuel by 2022. This goal could be surpassed by implementing perennial feedstock alone under scenario YR2022/$80 (72 billion L), or could be 90% met if the feedstock farm-gate price remained at $60 per dry ton under scenario YR2022/$60.

5.3 Green, Blue, and Gray Water Footprints

Green water requirements for growing perennial grass feedstock are derived from ET modeling (Section 4.3). The ET estimates for the perennial grasses were compared with ET assessment derived from remote sensing measurements [NTSG 2012]. Figure 4 presents a comparison between the estimated SWG ET and satellite imagery data for pasture/hay land. Notably, the resolutions of the adopted map layers are varied. The ET measurements are displayed at 8-km resolution, whereas the pasture/hay data are at 56-m resolution and calculated ET for SWG are at county level resolution with varying sizes. As such, results generated can be highly aggregated. Therefore, the satellite-image AET should be used as a reference instead of an absolute value set. With this limitation, we found that the projected switchgrass ET from our study falls within a reasonable range.

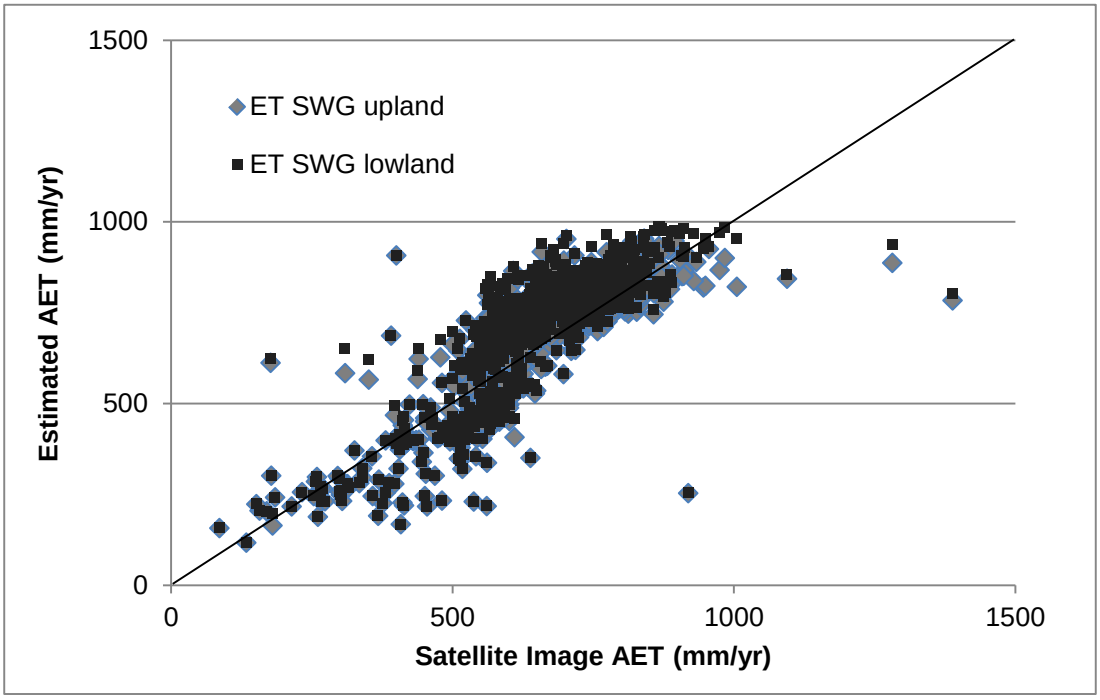

Figure 4 Estimated SWG AET from this study vs. values derived from satellite imagery.

Total green water required per volume of biofuel produced in each county for the six scenarios are presented in Figure 5(a)–(f). Green water is regulated by climate, type of feedstock, and biomass yield. The county-level green water intensities were in a dispersed pattern, with a minimum ranging from 529 L L^{-1} to 714 L L^{-1} and a maximum falling between 1644 L L^{-1} and 3,106 L L^{-1} for the six scenarios (Table 4). On a national weighted-average basis, the green water footprint ranged from 1,091 L L^{-1} to 1,170 L L^{-1} for the scenarios examined.

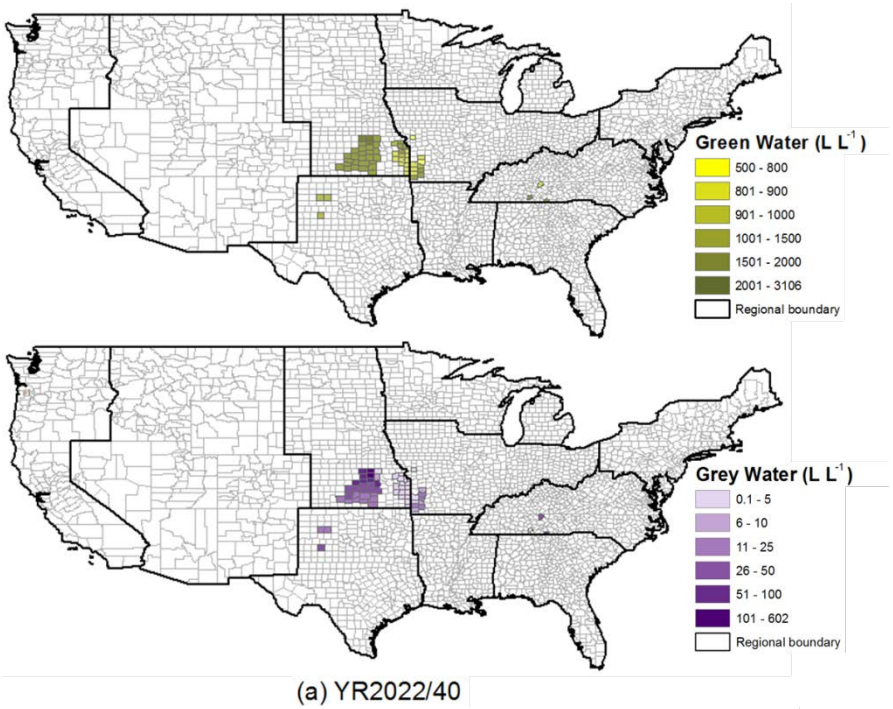

(a) YR2022/40

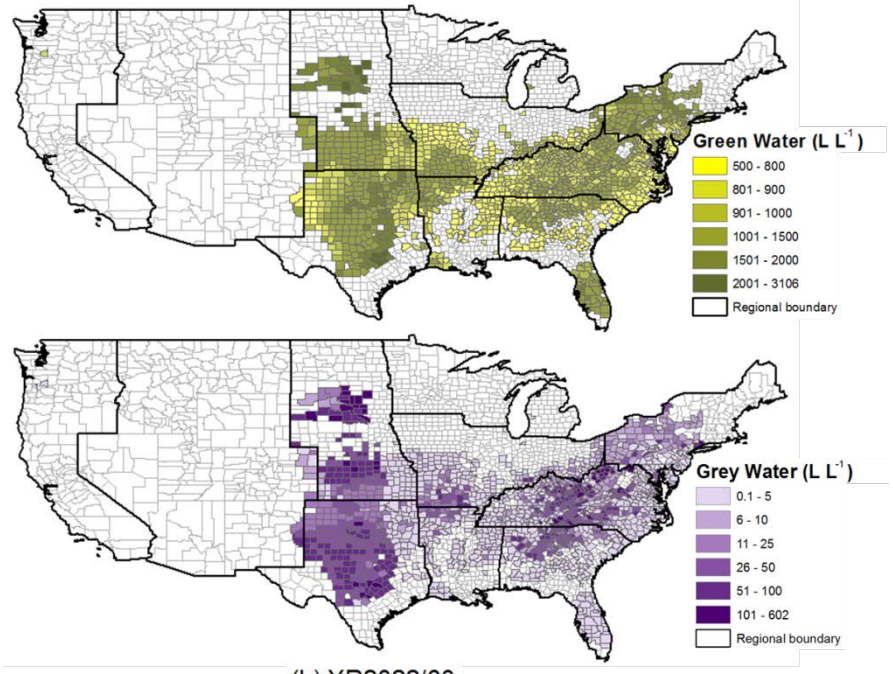

(b) YR2022/60

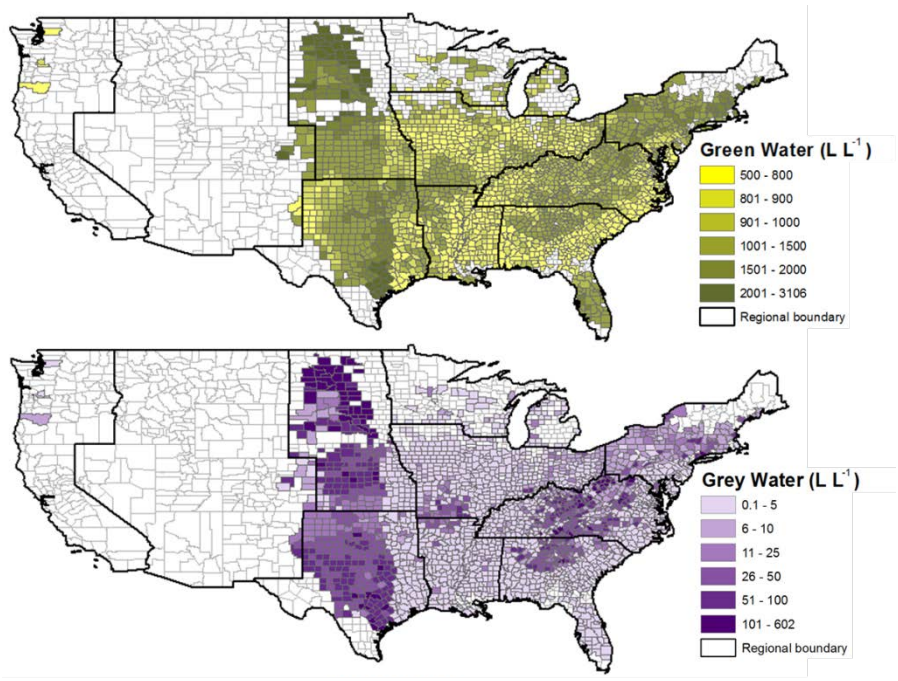

(c) YR2022/80

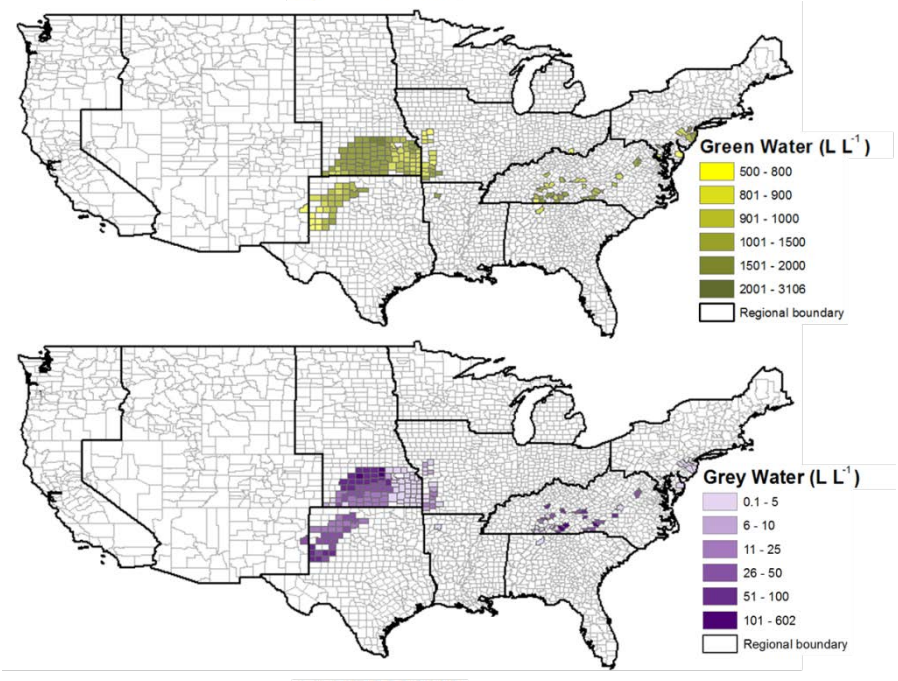

(d) YR2030/40

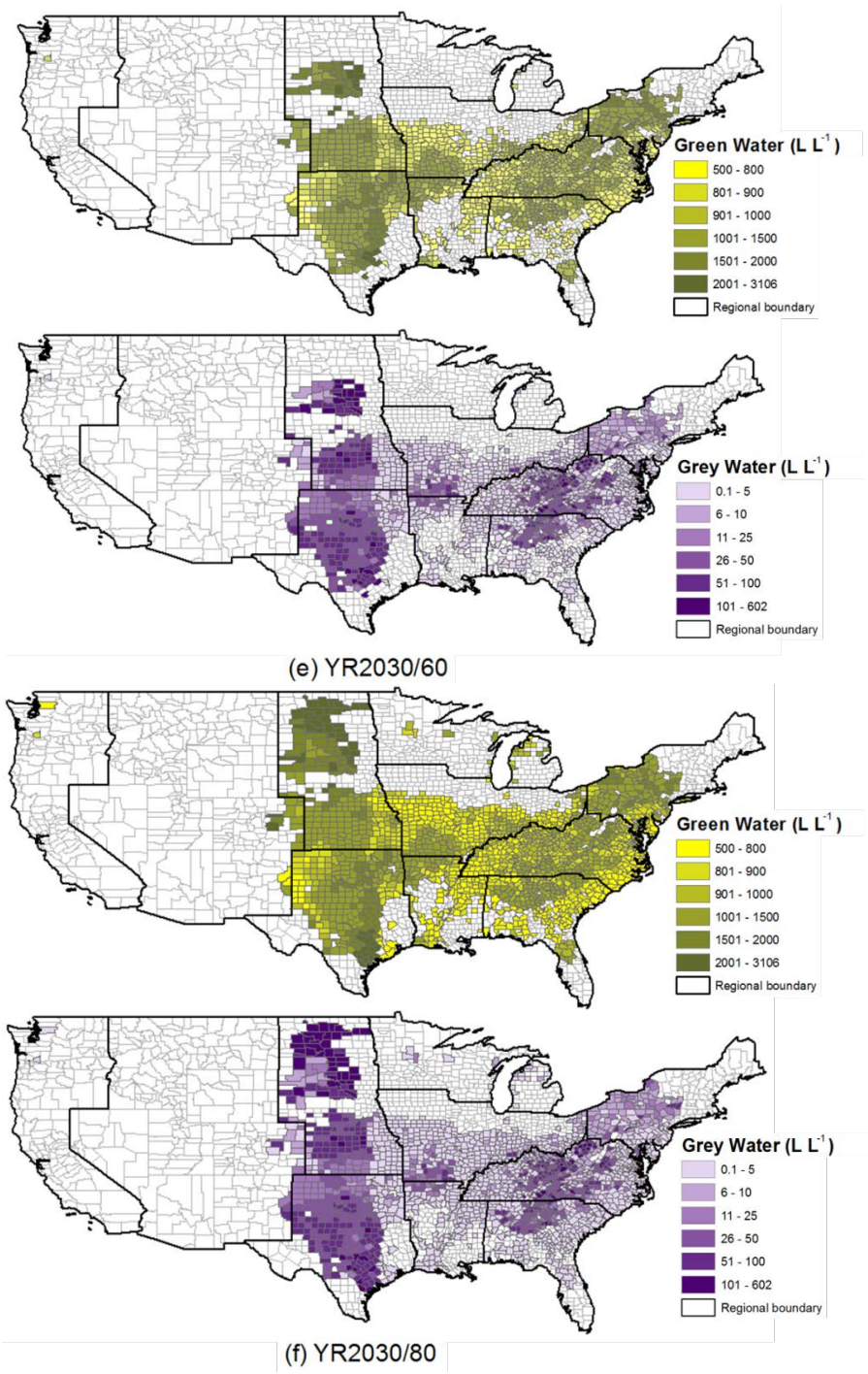

Figure 5 Green and gray water per liter of biofuel produced from perennial grass under six scenarios: (a) YR2022/40; (b) YR2022/60; (c) YR2022/80; (d) YR2030/40; (e) YR2030/60; (f) YR2030/80.

The patterns of gray water and green water footprint intensity are similar. The gray water footprint intensity depends largely on fertilizer application, soil condition, and grass yield, with substantial variances among locations. As shown in the YR2030/80 scenario (Figure 5), the high-intensity footprint is concentrated in the middle of the U.S., spreading from Texas to North Dakota, for both green and gray water. At the county level, the minimum values of the gray water footprint range from 0.06 L L^{-1} to 0.59 L L^{-1} whereas the maximums range from 150 L L^{-1} to 602 L L^{-1} for the six scenarios (Table 4). Weighted by feedstock production, the national average falls between 27 and 33 liters of gray water per liter of biofuel produced. This range of gray water footprints is rather small in comparison with other agricultural feedstock-based biofuels [Chiu and Wu 2012], and comparable to biofuels made from forest wood resources [Chiu and Wu 2013]. Research suggests that this amount can be further reduced by adopting agronomic management without applying fertilizer [Lemus et al. 2008].

Table 4 Statistical analysis of green, gray, and blue water footprints at the county level for the six scenarios

Scenario	YR2022/40	YR2022/60	YR2022/80	YR2030/40	YR2030/60	YR2030/80
	Green Water (L L^{-1})					
Maximum	1,644	2,308	3,106	1,644	2,308	3,106
Minimum	714	608	529	690	608	604
Weighted Average	1,170	1,104	1,115	1,091	1,106	1,140
Standard Deviation	154	559	558	238	557	593
	Blue Water (L L^{-1}) (update to 2 digits)					
Maximum	4.9	5.4	5.4	5.3	5.4	5.4
Minimum	4.2	2.7	2.7	4.2	2.7	2.7
Weighted Average	4.2	4.5	4.5	4.3	4.5	4.5
Standard Deviation	0.6	2.3	2.1	1.0	2.3	2.3
	Gray Water (L L^{-1})					
Maximum	150	554	602	271	554	602
Minimum	0.59	0.06	0.06	0.40	0.06	0.06
Weighted Average	29.58	27.44	28.01	33.30	26.91	29.48
Standard Deviation	5.37	29.48	36.55	10.53	30.07	35.51

When non-irrigated perennial grass is used as biofuel feedstock, the blue water footprint of the biofuel reflects biorefinery process water use and co-product water credit. For perennial

biofuel production via acid hydrolysis and fermentation, bioelectricity will be generated from lignin combustion. Thus, the amount of co-product water credit created in the process depends on the bioelectricity the refinery generates, the water consumed in generating the electricity, and the types of grid electricity mix it displaces. Since process water use does not vary with location, the variances of blue water will be governed by the regional grid electricity mix. Quantitatively, the water consumed in generating electricity is relatively small [Wu and Peng 2011]. Accounting for the water credit, the blue water footprint of biofuel produced from perennial grass ranges from 2.65 L L^{-1} to 5.40 L L^{-1} on the county level, with a production-weighted national average between 4.22 L L^{-1} (YR2022/40) and 4.52 L L^{-1} (YR2030/80) (Table 4). As water footprint data are aggregated from county to region to national level, their variability decreases.

5.4 Impact of Feedstock Mix

National weighted averages of green, blue and gray water footprints were further broken down by the type of grass feedstock for each of the six scenarios (Table 5). USWG has the highest green and gray water footprints among the three feedstocks. The green water footprint of USWG falls between 1878 and 2,161 L L^{-1}. This level of green water footprint is double that for MXG, which requires the lowest amount of green water per liter of biofuel produced. The national average gray water footprint of USWG biofuel is also highest among the three feedstocks under all scenarios, ranging from 128 to 136 L L^{-1}, 35 times greater than that of MXG biofuel (2.6–3.7 L L^{-1}). With respect to the intensity of their green and gray water footprints, the three feedstocks can be ranked as USWG > LSWG > MXG.

As the production scenarios progress from 2022 to 2030 and move toward higher feedstock prices—for example, from YR2022/40 to YR2022/60 to YR2022/80—an expansion of feedstock growing area is projected (Figure 2). Meanwhile, the feedstock type is extended from LSWG and MXG to include USWG in the portfolio. The feedstock composition in the region changes accordingly, and so does the water footprint. As a result, green and gray water footprints increase in the highest biomass production scenarios (YR2022/80 and YR2030/80).

Table 5 Comparison of water footprint per liter of biofuel produced for different grass types and scenarios

Scenario	YR2022/40	YR2022/60	YR2022/80	YR2030/40	YR2030/60	YR2030/80
	Blue Water Footprint (L L^{-1})					
USWG	-	3.40	4.20	-	3.40	4.27
USWG	4.21	4.50	4.55	4.37	4.51	4.55
MXG	4.26	4.46	4.52	4.28	4.46	4.50
	Green Water Footprint (L L^{-1})					
USWG	-	1,878	2,105	-	1,928	2,161
LSWG	1,235	1,230	1,282	1,150	1,245	1,299
MXG	986	953	917	927	946	924

Table 5 (Cont.)

Scenario	YR2022/40	YR2022/60	YR2022/80	YR2030/40	YR2030/60	YR2030/80
	Gray Water Footprint (L L^{-1})					
USWG	-	136	128	-	134	129
LSWG	39	47	50	44	47	50
MXG	3.7	3.7	3.5	2.6	3.7	3.6

A dominant factor influencing the distinct water footprint of each perennial grass is WUE. Presented as kilograms dry mass per hectare per centimeter of water consumed (kg ha^{-1} cm^{-1}), the WUE of perennial grass is closely related to both ET and biomass yield and is commonly adopted as a parameter to examine impacts on water resources. The high yield of MXG (Table 2) is likely a key reason it outperforms the relatively low-yield USWG. Though LSWG has a higher yield than USWG, it still requires a 41% higher green water footprint, and 46 more liters of gray water per liter of biofuel, than MXG under the YR2030/80 scenario. Using Central Illinois in the U.S. as an example, MXG exhibits a 39% higher ET than corn-soybean land in Illinois, whereas USWG appears to have a similar ET to a corn-soybean system [McIsaac et al. 2010]. Field studies indicate that the annual WUE of USWG falls between 55 and 97 kg ha^{-1} cm^{-1}, whereas that of MXG ranges from 90 to 191 kg ha^{-1} cm^{-1} [Hickman et al. 2010; Zeri et al. 2013]. These values can be higher if presenesced biomass is adopted to estimate WUE, resulting in a USWG WUE of 125 to over 500 and an MXG WUE of 320 to over 600 kg ha^{-1} cm^{-1} [Hickman et al. 2010; Zeri et al. 2013]. Another model simulation found that USWG and MXG grown in Illinois can reach WUE values ranging from 120 to 140 kg ha^{-1} cm^{-1} and 300 to 380 kg ha^{-1} cm^{-1}, respectively [Vanlooke et al. 2010]. In comparison, our study estimates the county-level WUEs of SWG and MXG in Illinois as ranging from 77 to 164 and 156 to 293 kg ha^{-1} cm^{-1}, respectively (Figure 6). The WUE for MXG is clearly at the high end. These ranges agree well with the field study results and fall in the middle of those from previous estimates. Figure 6 illustrates the widespread pattern of WUE for USWG, LSWG, and MXG. Regionally weighted WUEs for the feedstocks are presented in Table 6.

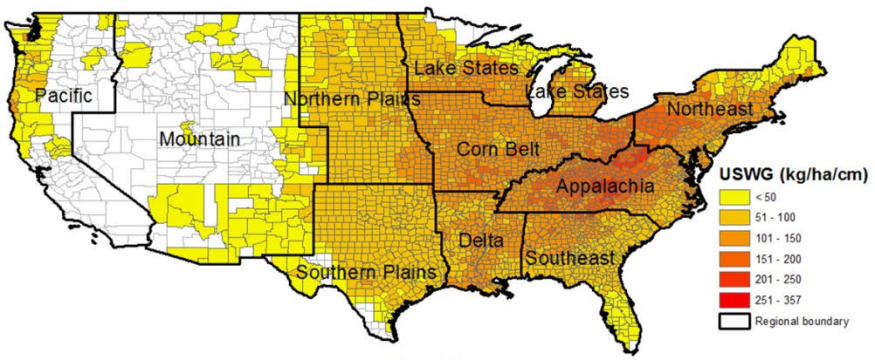

(a) USWG

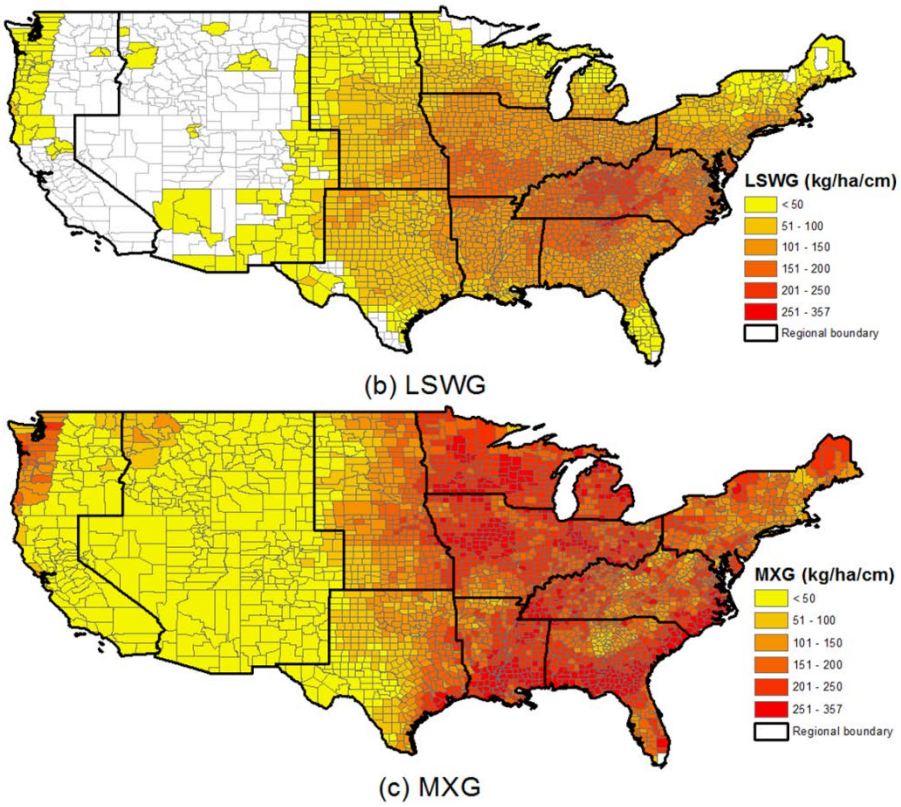

Figure 6 County-level WUE of the perennial grass in the U.S. in kg dry biomass per hectare per cm of green water for: (a) USWG, (b) LSWG, and (c) MXG.

Despite the high WUE of MXG, substantial amounts of fresh water would still be required annually to convert large areas of cropland to grow MXG. Vanlooke et al. [2010] indicated that a significant hydrological alteration may occur, especially in summer, if the land conversion ratio exceeds 25% in the Midwest region of the U.S.

Table 6 Annual WUE of USWG, LSWG, and MXG in the ten regions of the U.S.

Region	USWG	LSWG	MXG
	kg biomass/ha/cm water		
Northeast	121	103	160
Appalachia	144	175	194
Southeast	87	131	206
Delta	107	122	221
Corn Belt	129	139	217
Lake States	97	66	229

Table 6 (Cont.)

Region	USWG	LSWG	MXG
	kg biomass/ha/cm water		
Northern Plains	80	79	136
Southern Plains	67	79	106
Mountain	12	10	22
Pacific	14	6	51

5.5 Comparison of the Scenarios

Analysis of the standard deviations of county-level green and gray water footprints for the six scenarios reveals small variations in the YR2022/40 and YR2030/40 scenarios. The deviations increase as the scenarios shift to YR2022/80 and YR2030/80 (Table 4). The escalation of variances in green and gray water footprint indicates a change in feedstock composition and geographic area as the land conversion is expanded to more low-productivity land. In particular, the land conversion can involve some counties that do not show water-footprint advantages. Factoring in climate and soil conditions, there could be substantial yield variability when a given feedstock is grown in different regions (Table 2). This trend in the six scenarios is expected because the scenarios were primarily developed on the basis of market, economics, and land productivity for the feedstock resources. As the market develops and the demand increases and more land conversions occur, the water footprint will be altered accordingly.

Nationally, there is an upward trend of green water footprints for SWG from 2022 to 2030 (Table 5) and no clear trend for MXG. At the mixed feedstock level for each scenario, however, we noticed an increase in green and gray water footprint from $60 per dry ton to $80 per dry ton for both year 2022 and 2030 (Table 4). At regional level, the total water footprint (the sum of blue, green, and gray water) does not show a consistent pattern and strong correlation in responding to the scenarios across different regions (Figure 7). Each region may show very distinctive fluctuations in water footprint. For instance, the water footprint in the Northern and Southern Plains shows positive correlation with the scenarios from YR2022/40 to YR2022/80 or from YR2030/40 to YR2030/80, whereas those in the Corn Belt, Delta, and Pacific regions show negative correlations. Figure 7 further illustrates that the scenarios were not optimized for water footprint.

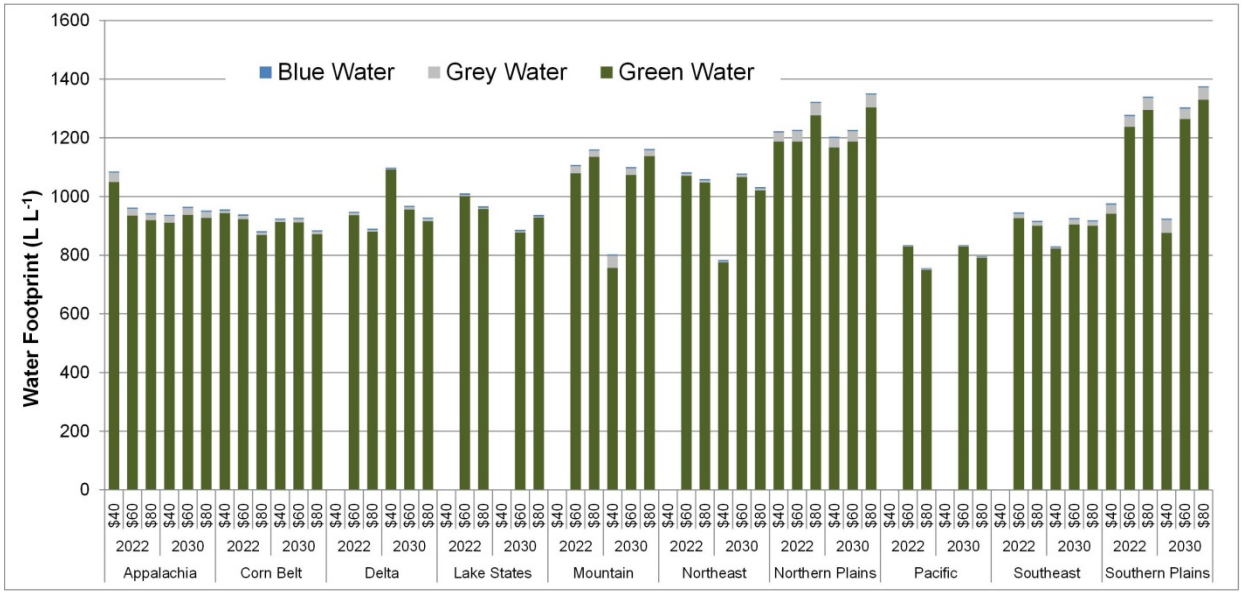

Figure 7 Water footprint of biofuel produced from perennial grass under different scenarios in ten U.S. agricultural resource regions. (See Table 1 for scenario details.)

5.6 Implications for Water Resources

We derived a quantitative indicator—blue and green water resource index (BGI) — showing the fraction of total blue and green water volume in total annual precipitation, to represent the use of renewable water resources or precipitation appropriation schemes. The result shows that the grass-based biofuel accounts for proportions ranging from a trace up to 6% of annual precipitation at the regional level, depending on production scenario and location. At the county level, the BGI could vary substantially and reach significantly higher values, as expected (Figure 8). Using the scenario YR2030/80 as an example, the highest precipitation appropriation was estimated to be 30% in the Central region of the U.S., with a cluster of neighboring high-water-appropriation counties (Figure 8). Overall, a significant increase in water resources appropriation is observed from YR2022/40 or YR2030/40 to YR2022/60 or YR2030/60 (Figure 8), as total biomass production volume increases dramatically (Table 3).

The effects of blue water in appropriating annual precipitation resources are minimal and account for only 0.09% of local precipitation at most, as the feedstock receives no irrigation water. Blue water use in biorefineries is typically sourced from local groundwater because of its desirable consistency in water quality. Groundwater resources can be shallow or deep. The shallow groundwater source is accounted for in this study because it is connected to surface water and indirectly replenished through precipitation. Groundwater pumped from deep aquifer (non-renewable water) represents a net loss of water stock in the region. The county-level water resource estimate assumes a distributed biofuel production. In reality, biorefineries are likely to be centrally located and built at a sufficient scale to be economically feasible, and to acquire feedstock from several neighboring areas/counties. A 50-million-gal (189-million-L)-per-year biorefinery would require 250 million gal (946 million L) of groundwater annually (at a yield of

5 L biofuel per L feedstock). Therefore, the water resource needs in one refinery (blue water) at a given location could be substantial, representing the sum of the groundwater needs for processing all of the feedstock in the plant capacity. Further, a cluster of biorefineries located in several neighboring counties or states can also account for additional stress on local groundwater resources. In both cases, the water table could decrease if biorefinery planning did not include careful selection of local water resources. This study does not focus on groundwater resources. Nevertheless, it clearly shows that biorefineries have an important impact on water resources even though the overall blue water allocation for annual precipitation is small.

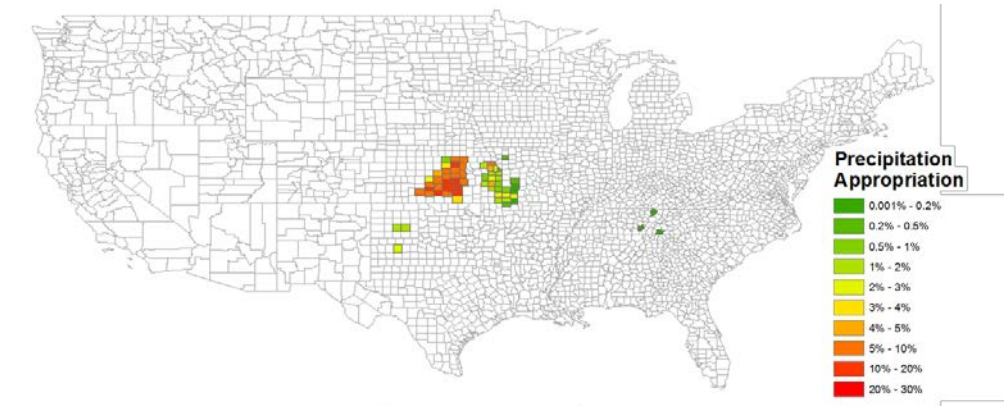

(a) YR2022/40

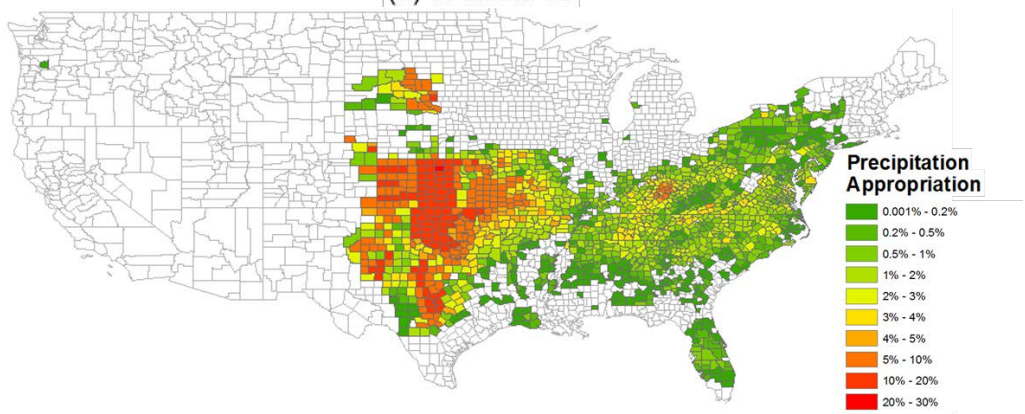

(b) YR2022/60

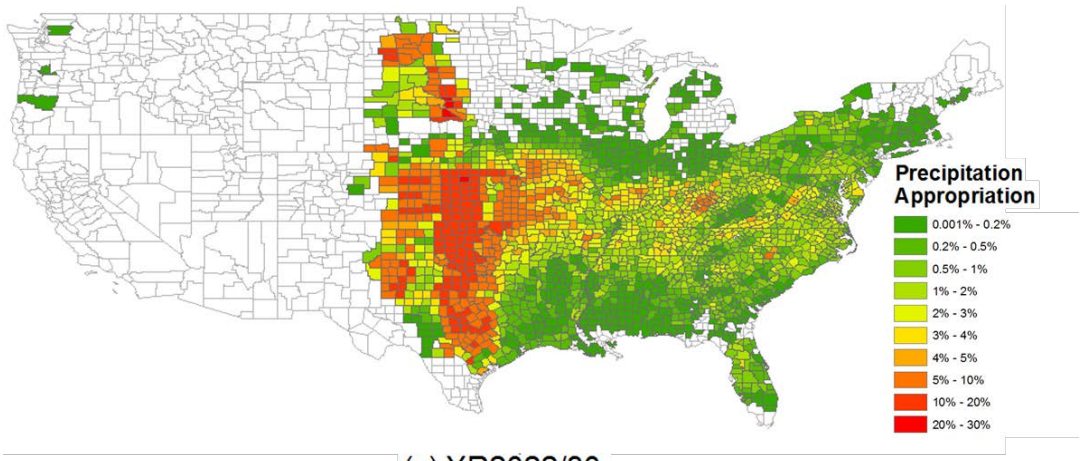

(c) YR2022/80

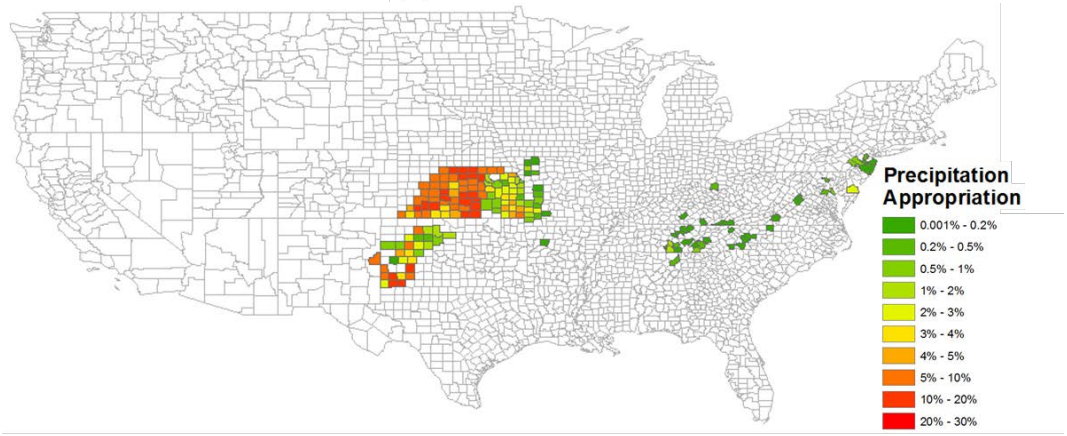

(d) YR2030/40

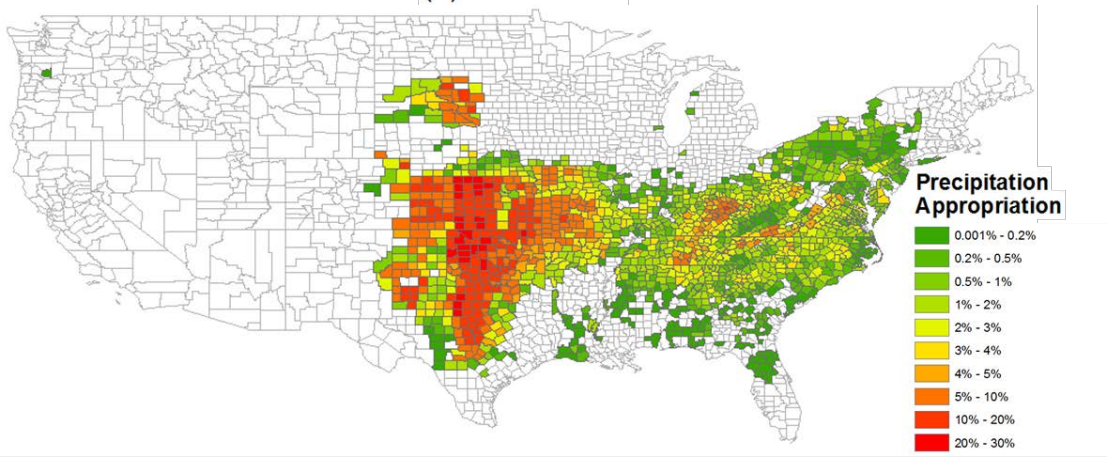

(e) YR2030/60

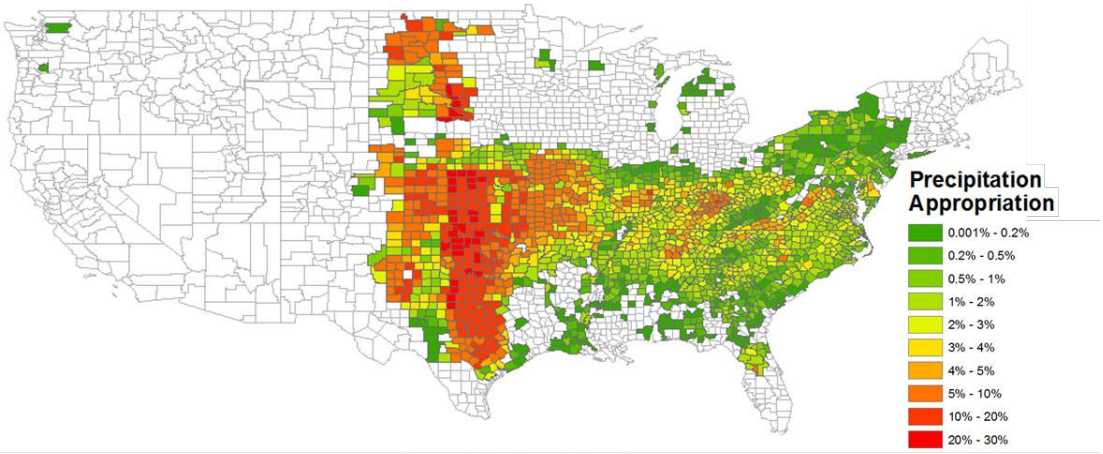

Figure 8 Water resource appropriation index BGI for grass-based biofuel on a county level under the scenarios of: (a) YR2022/40; (b) YR2022/60; (c) YR2022/80; (d) YR2030/40; (e) YR2030/60; (f) YR2030/80.

6 UNCERTAINTIES

Currently, there is no large-scale grass plantation dedicated to biofuel production in the United States. The results of this study indicate the expected level of water footprint associated with each type of grass in the selected counties "if" it is to be grown. Several factors contribute to uncertainties in the results. First is the simplified assumption of the feedstock mix. Because the projected feedstock production does not specify the grass ecotypes or species, our grass selection mechanism (see Section 2) reflects the potential grass productivity based on the grass candidate with the relatively highest yield, which consequently requires less land. We also assume that in each designated county, only the type of grass with the highest yield would be grown for biofuel feedstock. However, in reality, a perennial feedstock mix with similar yield is likely to be grown in each of the participating counties. Second, the grass yields are projected under ideal conditions. Once the assumptions of environmental stress and agricultural practices are altered, the yields can vary significantly, directly leading to a change in water footprint.

This study focuses only on non-irrigated perennial grass. It projects the biomass productivity potential with an assumption of no irrigation. A former study found that water stress can have a significant impact on the above-ground biomass of MXG [Clifton-Brown and Lewandowski 2000]. Therefore, this assumption can lead to possible underestimation of blue water. Unfortunately, field data to verify biomass growth under water stress in the designated growing regions are lacking. In terms of gray water, the current simulation applies exactly the same amount of fertilizer per growing area for all types of grass, because of the field data limitation. This quantity can be varied by region and should be further improved when more field data become available.

7 CONCLUSIONS

This study illustrates the county-level water footprints associated with biofuel production from perennial grasses, highlights the interconnection between land use and water footprints, and demonstrates the geographical deviations of water footprints under different feedstock production scenarios. Depending on the regions selected, the non-crop land requirement and water resource acquisition needs can be substantial. Under the scenarios examined, a total (area-weighted average) of 2.15–2.39 m^2 of land area is required to produce a liter of cellulosic biofuel from perennial grasses. With the scenario YR22/80, 219 million metric ton of perennial grass feedstoick can be grown in the U.S. by 2022, enough to produce up to 72 billion L (19 billion gal) of cellulosic biofuel—surpassing the EISA goal by 3 billion gallons. On (a nationally weighted) average, the green water footprint ranged from 1,091 L L-1 to 1,170 L L-1, blue water from 4.22 L L-1 to 4.52 L L-1, and gray water from 27 to 33 L L-1. This gray-water footprint range is comparable to that of biofuel based on forest wood resources.

USWG has the highest green and gray water footprint among the three feedstocks and double that for MXG, which requires the lowest green water footprint. The intensity of green and gray water footprints for the three feedstocks studied can be ranked as USWG > LSWG > MXG. The state, regional, and national water footprints associated with each type of grass can fluctuate under different feedstock production scenarios as a consequence of spatial aggregation of land conversion. As water footprint data are aggregated from a county to a regional to a national level, their variability decreases. There is no consistent pattern in water footprint for the production regions in the U.S. across the six scenarios studied.

From the water resource appropriation perspective, grass-based biofuel accounts for amounts ranging from a trace up to 6% of annual precipitation at the regional level, depending on production scenario and location. At the county level, the BGI could vary substantially and reach significantly higher values. Results from this study can inform decision-makers and assist in feedstock production planning by taking local climate, feedstock water demands, the biomass mix, and regional water resource availability into account.

REFERENCES

Adler, P.R., S.J. Del Grosso, and W.J. Parton (2007). "Life-cycle assessment of net greenhouse-gas flux for bioenergy cropping systems." *Ecological Applications* 17(3):675–691.

Allen, R.G., L.S. Pereira, D. Raes, and M. Smith (1998). Crop evapotranspiration: Guidelines for computing crop water requirements. Food and Agriculture Organization of the United Nations, Rome: *Irrigation and Drainage* Paper 56.

Angelini, L.G., L. Ceccarini, N. Nassi o Di Nasso, and E. Bonari (2009). "Comparison of Arundo donax L. and *Miscanthus* × *giganteus* in a long-term field experiment in central Italy: Analysis of productive characteristics and energy balance." *Biomass and Bioenergy* 33(4):635–643.

Beale, C.V., J.I.L. Morison, and S.P. Long (1999). "Water use efficiency of C4 perennial grasses in a temperate climate." *Agricultural and Forest Meteorology* 96(1–3):103–115.

Berndes, G. (2002). "Bioenergy and water — the implications of large-scale bioenergy production for water use and supply." *Global Environmental Change* 12(4):253–271.

Chapagain, A.K., and A.Y. Hoekstra (2004). Water Footprints of Nations, Value of Water Research Report, Series No. 16, Vols. 1 and 2, UNESCO-IHE, Delft.

Chiu, Y.-W., and M. Wu (2012). "Assessing county-level water footprints of different cellulosic-biofuel feedstock pathways." *Environmental Science & Technology* 46(16):9155–9162.

Chiu, Y. and Wu, M. (2013a). "The water footprint of biofuel produced from forest wood residue via a mixed alcohol gasification process." *Environ. Res. Lett.* 8 (2013), doi:10.1088/1748–9326/8/3/035015.

Chiu, Y. and Wu, M. (2013b). Considering water availability and wastewater resources in the development of algal bio-oil, *Biofuels, Bioprod. Bioref.* (2013) Vol. 7 (4), p406-415. DOI: 10.1002/bbb.1397.

Chiu, Y., B. Walseth, and S. Suh (2009), Water embodied in bioethanol in the United States, *Environ. Sci. Technol*. 43(8), 2688–2692.

Christian, D.G., A.B. Riche, and N.E. Yates (2008). "Growth, yield and mineral content of *Miscanthus* × *giganteus* grown as a biofuel for 14 successive harvests." *Industrial Crops and Products* 28(3):320–327.

Clifton-Brown, J.C., and I. Lewandowski (2000). "Water use efficiency and biomass partitioning of three different *Miscanthus* genotypes with limited and unlimited water supply." *Annals of Botany* 86(1):191–200.

Collins, M. (1994). Biomass Production by Fescue and Switchgrass Alone and in Mixed Swards with Legumes. Final Project Report, ORNL/Sub-88-SC617, Oak Ridge National Laboratory, Oak Ridge, TN, p. 101.

David, K., and A.J. Ragauskas (2010). "Switchgrass as an energy crop for biofuel production: A review of its ligno-cellulosic chemical properties." *Energy & Environmental Science* 3(9):1182–1190.

De La Torre Ugarte, D.G., L. He, K.L. Jensen, and B.C. English (2010). "Expanded biofuel production: Implications for agriculture, water demand, and water quality." *Biomass and Bioenergy* 34(11):1586–1596.

Dohleman, F.G., E.A. Heaton, R.A. Arundale, and S.P. Long (2012). "Seasonal dynamics of above- and below-ground biomass and nitrogen partitioning in *Miscanthus* × *giganteus* and Panicum virgatum across three growing seasons." *GCB Bioenergy* 4(5):534–544. DOI 10.1111/j.1757–1707.2011.01153.x.

Dominguez-Faus, R., S.E. Powers, J.G. Burken, and P.J. Alvarez (2009). "The water footprint of biofuels: A drink or drive issue?" *Environmental Science & Technology* 43(9):3005–3010.

Evans, J.M., and M.J. Cohen (2009). Regional Water Resource Implications of Bioethanol Production in the Southeastern United States, *Glob. Change Biol.*, 15(9), 2261–2273, doi: DOI: 10.1111/j.1365-2486.2009.01868.x.

Fargione, J., J. Hill, D. Tilman, S. Polasky, and P. Hawthorne (2008). "Land clearing and the biofuel carbon debt." Science 319(5867):1235–1238.

Fingerman, K.R.G. Berndes, St. Orr, B.D. Richter, P. Vugteveen (2011). "Impact assessment at the bioenergy-water nexus." Biofuels, Bioprod. Bioref. 5:375–386.

Gerbens-Leenes, P.W., A.Y. Hoekstra, and T.H. van der Meer (2009). The Water Footprint of Bioenergy, *Proc. Natl. Acad. Sci*., 106(25), 10219–10223.

Gerbens-Leenes, P.W., and A.Y. Hoekstra (2009). The Water Footprint of Sweeteners and Bio-Ethanol from Sugar Cane, Sugar Beet, and Maize, Research Reports Series No. 38, UNESCO-IHE Institute of Water Education, Nov.

Glover, J.D., S.W. Culman, S.T. DuPont, W. Broussard, L. Young, M.E. Mangan, J.G. Mai, T.E. Crews, L.R. DeHaan, D.H. Buckley, H. Ferris, R.E. Turner, H.L. Reynolds, and D.L. Wyse (2010). "Harvested perennial grasslands provide ecological benchmarks for agricultural sustainability." *Agriculture, Ecosystems & Environment* 137(1–2):3–12.

Gunderson, C.A., E.B. Davis, H.I. Jager, T.O. West, R.D. Perlack, C.C. Brandt, S.D. Wullschleger, L.M. Baskaran, E.G. Wilkerson, and M.E. Downing (2008). Exploring Potential U.S. Switchgrass Production for Lignocellulosic Ethanol, ORNL/TM-2007/183, Oak Ridge National Laboratory, Oak Ridge, TN.

Heaton, E.A., F.G. Dohleman, and S.P. Long (2008). “Meeting US biofuel goals with less land: The potential of *Miscanthus*.” *Global Change Biology* 14(9):2000–2014.

Heaton, E.A., F.G. Dohleman, A.F. Miguez, J.A. Juvik, V. Lozovaya, J. Widholm, O.A. Zabotina, G.F.McIsaac, M.B. David, T.B. Voigt, N.N. Boersma, and S.P. Long (2010). *Miscanthus*: A promising biomass crop. *Advances in Botanical Research*, ed. J.-C. Kader and M. Delseny, 56:75–124. London: Academic Press.

Hickman, G.C., A. Vanloocke, F.G. Dohleman, and C.J. Bernacchi (2010). “A comparison of canopy evapotranspiration for maize and two perennial grasses identified as potential bioenergy crops.” *Global Change Biology* 2(4):157–168.

Hoekstra, A.Y., A.K. Chapagain, M.M. Aldaya, and M.M. Mekonnen (2011). The Water Footprint Assessment Manual: Setting the Global Standard. London: Earthscan.

Hohenstein, W.G., and L.L. Wright (1994). “Biomass energy production in the United States: An overview.” *Biomass and Bioenergy* 6(3):161–173.

Huang, Y., D.H. Rickerl, and K.D. Kephart (1996). “Recovery of deep-point injected soil nitrogen-15 by switchgrass, alfalfa, ineffective alfalfa, and corn.” *Journal of Environmental Quality* 25(6):1394–1400.

Humbird, D., R. Davis, L. Tao, C. Kinchin, D. Hsu, and A. Aden (2011), Process Design and Economics for Biochemical Conversion of Lignocellulosic Biomass to Ethanol, National Renewable Energy Laboratory Report NREL/TP-5100-47664, May.

ISO 14046:2014 (2014). “Environmental management -- Water footprint -- Principles, requirements and guidelines.” Available at http://www.iso.org/iso/home/store/catalogue_tc/catalogue_detail.htm?csnumber=43263. Accessed Oct. 2, 2014.

Jacovides, C.P., F.S. Tymvios, D.N. Asimakopoulos, K.M. Theofilou, and S. Pashiardes (2003). “Global photosynthetically active radiation and its relationship with global solar radiation in the Eastern Mediterranean basin.” *Theoretical and Applied Climatology* 74(3–4):227–233.

Jager, H.I., L.M. Baskaran, C.C. Brandt, E.B. Davis, C.A. Gunderson, and S.D. Wullschleger (2010). “Empirical geographic modeling of switchgrass yields in the United States.” *Global Change Biology* 2(5):248–257.

King, C.W., and M.E. Webber (2008). Water Intensity of Transportation, *Environ. Sci. Technol.*, 42(21), 7866–7872.

Kiniry, J.R., M.V.V. Johnson, S.B. Bruckerhoff, J.U. Kaiser, R.L. Cordsiemon, and R.D. Harmel (2012). “Clash of the Titans: Comparing productivity via radiation use efficiency for two grass giants of the biofuel field.” *BioEnergy Research* 5(1):41–48.

Lemus, R., E.C. Brummer, C.L. Burras, K.J. Moore, M.F. Barker, and N.E. Molstad (2008). "Effects of nitrogen fertilization on biomass yield and quality in large fields of established switchgrass in southern Iowa, USA." *Biomass and Bioenergy* 32(12):1187–1194.

Lewandowski, I., J.C. Clifton-Brown, J.M.O. Scurlock, and W. Huisman (2000). "*Miscanthus*: European experience with a novel energy crop." *Biomass and Bioenergy* 19(4):209–227.

McIsaac, G.F., M.B. David, and C.A. Mitchell (2010). "*Miscanthus* and switchgrass production in central Illinois: Impacts on hydrology and inorganic nitrogen leaching." *Journal of Environmental Quality* 39:1790–1799.

McIsaac, G.F. (2014). "Biomass Production and Water: A Brief Review of Recent Research," Current Sustainable/Renewable Energy Reports Online publish: Sept. 24. DOI: 10.1007/s40518-014-0016-3.

McLaughlin, S.B., and L. Adams Kszos (2005). "Development of switchgrass (Panicum virgatum) as a bioenergy feedstock in the United States." *Biomass and Bioenergy* 28(6):515–535.

McLaughlin, S.B., J.R. Kiniry, C.M. Taliaferro ,and D. De La Torre Ugarte (2006). Projecting yield and utilization potential of switchgrass as an energy crop. *Advances in Agronomy*, ed. L.S. Donald, 90:267–297. London: Academic Press.

Miguez, F.E., M. Maughan, G.A. Bollero, and S.P. Long (2012). "Modeling spatial and dynamic variation in growth, yield, and yield stability of the bioenergy crops *Miscanthus* × *giganteus* and Panicum virgatum across the conterminous United States." *Global Change Biology* 4(5):509–520.

Mishra, G.S., and S. Yeh (2011), Life Cycle Water Consumption and Withdrawal Requirements of Ethanol from Corn Grain and Residues, *Environ. Sci. Technol.*, 45(10), 4563–4569

Naidu, S.L., S.P. Moose, A.K. AL-Shoaibi, C.A. Raines, and S.P. Long (2003). "Cold tolerance of C4 photosynthesis in *Miscanthus* × *giganteus*: Adaptation in amounts and sequence of C4 photosynthetic enzymes." *Plant Physiology* 132(3):1688–1697.

Neitsch, S.L., J.G. Arnold, J.R. Kiniry, and J.R. Williams (2011). Soil and Water Assessment Tool, Theoretical Documentation, Version 2009, TR-406, Texas A&M University, College Station, TX, p. 647.

Nouvellon, Y., D.L. Seen, S. Rambal, A. Bégué, M.S. Moran, Y. Kerr, and J. Qi (2000). "Time course of radiation use efficiency in a shortgrass ecosystem: Consequences for remotely sensed estimation of primary production." *Remote Sensing of Environment* 71(1):43–55.

NTSG (Numerical Terradynamic Simulation Group) (2012). "Hydrology - Global Evapotranspiration." Retrieved 05/16/12 from http://www.ntsg.umt.edu/data. Global 8km resolution.

Nyakatawa, E.Z., D.A. Mays, V.R. Tolbert, T.H. Green, and L. Bingham (2006). "Runoff, sediment, nitrogen, and phosphorus losses from agricultural land converted to sweetgum and switchgrass bioenergy feedstock production in north Alabama." *Biomass & Bioenergy* 30(7):655–664.

ORNL (Oak Ridge National Laboratory) (2011). Distributed Active Archive Center for Biogeochemical Dynamics. Retrieved 9/28/14 from http://webmap.ornl.gov/wcsdown/dataset.jsp?ds_id=569.

Price, L., M. Bullard, H. Lyons, S. Anthony, and P. Nixon (2004). "Identifying the yield potential of *Miscanthus* × *giganteus*: An assessment of the spatial and temporal variability of *M. x giganteus* biomass productivity across England and Wales." *Biomass and Bioenergy* 26(1):3–13.

Schmer, M.R., K.P. Vogel, R.B. Mitchell, and R.K. Perrin (2008). "Net energy of cellulosic ethanol from switchgrass." *Proceedings of the National Academy of Sciences* 105(2):464–469.

Schmitt, M.A., C.C. Sheaffer, and G.W. Randall (1994). "Manure and fertilizer effects on alfalfa plant nitrogen and soil nitrogen." *Journal of Production Agriculture* 7(1):104–109.

Scown, C.D., A. Horvath, and T.E. McKone (2011). Water Footprint of U.S. Transportation Fuels, *Environ. Sci. Technol.* 45(7), 2541–2553.

Smith, R.A., R.B. Alexander, and G.E. Schwarz (2003). "Natural background concentrations of nutrients in streams and rivers of the conterminous United States." *Environmental Science & Technology* 37(14):3039–3047.

Staples, M.D., H. Olcay, R. Malina, P. Trivedi, M.N. Pearlson, K. Strzepek, S.V. Paltsev, C. Wollersheim, and S.R.H. Barrett (2013). "Water Consumption Footprint and Land Requirements of Large-Scale Alternative Diesel and Jet Fuel Production." Environ, Sci, & Technol, 47(21), pp 12557–12565. dx.doi.org/10.1021/es4030782.

Stout, W.L. (1992). "Water-use efficiency of grasses as affected by soil, nitrogen, and temperature." *Soil Science Society of America Journal* 56(3):897–902.

Tilman, D., J. Hill, and C. Lehman (2006). "Carbon-negative biofuels from low-input high-diversity grassland biomass." *Science* 314(5805):1598–1600.

USDA (U.S. Department of Agriculture) (2010). "Cropland Data Layer." National Agricultural Statistics Service. Retrieved 09/01/11 from http://www.nass.usda.gov/research/Cropland/SARS1a.htm.

USDA NRCS (Natural Resources Conservation Service) (2012). "Plants Database." Retrieved 3/12/12 from http://plants.usda.gov.

USDOE (U.S. Department of Energy) (2006). Breaking the Biological Barriers to Cellulosic Ethanol: A Joint Research Agenda, DOE/SC-0095, U.S. DOE Office of Science and Office of Energy Efficiency and Renewable Energy, Washington, D.C.

USDOE (2011). U.S. Billion-Ton Update: Biomass Supply for a Bioenergy and Bioproducts Industry. R.D. Perlack and B.J. Stokes (Leads), ORNL/TM-2011/224, Oak Ridge National Laboratory, Oak Ridge, TN. http://www1.eere.energy.gov/biomass/pdfs/billion_ton_update.pdf, accessed April 2012.

USEPA (U.S. Environmental Protection Agency) (1992). Safe Drinking Water Act (SDWA). Retrieved 9/28/14 from http://water.epa.gov/lawsregs/rulesregs/sdwa/index.cfm.

USGS (U.S. Geological Survey) (2011). SPARROW Decision Support System 1992 Total Nitrogen Model for the Conterminous U.S. Retrieved 11/15/11 from http://cida.usgs.gov/sparrow/map.jsp?model=22.

Vanloocke, A., C.J. Bernacchi, and T.E. Twine (2010). "The impacts of *Miscanthus* × *giganteus* production on the Midwest US hydrologic cycle." *Global Change Biology* 2(4):180–191.

Vogel, K.P., and R.B. Mitchell (2008). "Heterosis in switchgrass: Biomass yield in swards." *Crop Science* 48(6):2159–2164.

Wu, M., Z. Zhang, Y. Chiu (2014). Life-cycle Water Quantity and Water Quality Implications of Biofuels, *Current Reports special issues: Current Sustainable/Renewable Energy Reports*. 1: 3–10. DOI 10.1007/s40518-013-0001-2, e-ISSN 2196-3010.

Wu, M., Y. Chiu, and Y. Demissie (2012a). "Quantifying the regional water footprint of biofuel production by incorporating hydrologic modeling." *Water Resources Research* 48(10):W10518.

Wu, M., Y. Demissie, and E. Yan (2012), Simulated Impact of Future Biofuel Production on Water Quality and Water Cycle Dynamics in the Upper Mississippi River Basin, *Biomass Bioenergy*, 41(2012), 44–56.

Wu, M., and Peng, J. (2011). Developing a Tool to Estimate Water Use in Electric Power Generation in the United States, ANL/ESD/11–2 ― Update, Argonne National Laboratory, Argonne, IL.

Wu, M., M. Mintz, M. Wang, and S. Arora (2009). Water Consumption in the Production of Ethanol and Petroleum Gasoline, *Environ. Manage.*, 44(5), 981–997.

Wu, M., Y. Wu, and M. Wang (2006). "Energy and emission benefits of alternative transportation liquid fuels derived from switchgrass: A fuel life cycle assessment." *Biotechnology Progress* 22(4):1012–1024.

Zegada-Lizarazu, W., S. Wullschleger, S.S. Nair, and A. Monti (2012). “Crop physiology,” pp. 55–86 in: Switchgrass: A Valuable Biomass Crop for Energy. ed. A. Monti. London: Springer Verlag.

Zeri, M., M.Z. Hussain, K.J. Anderson-Teixeira, E. DeLucia, and C.J. Bernacchi (2013). “Water use efficiency of perennial and annual bioenergy crops in central Illinois.” Journal of Geophysical Research: Biogeosciences 118(2):581–589.